Construction and Building Materials 324 (2022) 126628

Contents lists available at ScienceDirect

Construction and Building Materials

journal homepage: www.elsevier.com/locate/conbuildmat

Shape memory alloy reinforcement for strengthening and self-centering of concrete structures—State of the art

Saim Raza [a], Behrouz Shafei [a,b], M. Saiid Saiidi [c], Masoud Motavalli [a,d], Moslem Shahverdi [a,d,*]

[a] Empa, Swiss Federal Laboratories for Materials Science and Technology, Dübendorf 8600, Switzerland
[b] Department of Civil, Construction, and Environmental Engineering, Iowa State University, Ames, IA 50011, United States
[c] Department of Civil and Environmental Engineering, University of Nevada, Reno, Reno, NV 89557, United States
[d] School of Civil Engineering, University of Tehran, Tehran 4563-11155, Iran

ARTICLE INFO

Keywords:
Shape memory alloys
Reinforced concrete structures
Flexural strengthening
Shear strengthening
Self-centering, New reinforcement

ABSTRACT

The degradation of reinforced concrete (RC) structural components owing to aging mechanisms and extreme loading events can cause significant performance and safety concerns. Among the available alternatives for restoring such components, shape memory alloys (SMAs) exhibit unique properties, including the recovery of inelastic strain upon unloading (superelasticity) and/or heating (shape memory effect, SME). Particularly, the superelasticity and SME of SMAs can be applied to reduce permanent deformations and incorporate self-centering behavior into RC structures. Furthermore, the addition of SMAs can enhance the strength and stiffness of RC structures, enabling them to resist high load intensities with less damage. Despite the variety of investigations conducted on the structural applications of SMAs, the existing literature lacks a holistic review of the current progress, main findings, potential limitations, and future prospects of SMAs for the strengthening of existing RC structures and the design of new ones. Furthermore, comprehensive guidance is missing for selecting the SMA types and characteristics most suitable for a particular strengthening/self-centering application. To address the identified fundamental and practical gaps, we performed a detailed review of the applications of SMAs in RC beams, columns, beam-column joints, and shear walls. The identified applications were explored from the perspective of the self-centering, crack recovery, strength enhancement, confinement, and shear strengthening of existing and new RC structures. A critical review of the advantages and disadvantages of strengthening with SMAs is then provided, especially in comparison to conventional strengthening materials and methods. This review concludes with the identification of challenges associated with using SMAs and future opportunities that can arise owing to the proper use of SMAs.

1. Introduction

Reinforced concrete (RC) structures can experience excessive damage owing to aging and extreme loading events. The incurred damage is often a combination of cracking and spalling of concrete, and may further lead to corrosion, fracture, and buckling of embedded steel rebars. As a result, the strength and serviceability of RC structures can be adversely affected, leading to short- and long-term performance and safety concerns. To address these concerns, various strengthening and repair materials have been developed, including corrosion-resistant steel plates, high-performance cementitious composites, externally bonded fiber-reinforced polymer (FRP) jackets, and near-surface-mounted (NSM) FRP sheets [1–4]. In addition to the aforenoted alternatives, shape memory alloys (SMAs) are being applied for the strengthening and repair of RC structures owing to their unique properties, that is, superelasticity and the shape memory effect (SME) [5–6]. Because of superelasticity, SMAs can return to their original undeformed shape on unloading after experiencing large deformations. On the other hand, the SME provides the response characteristic, whereby upon heating, the SMAs can recover their inelastic strains after large deformations. Furthermore, SMAs have a relatively easy installation process, particularly for prestressing applications. These properties make SMAs an attractive alternative not only for strengthening and repair but also for the design of new structures, especially where the primary objective is to reduce residual deformations and maintain the functionality of RC structures after an extreme loading event.

* Corresponding author.
E-mail addresses: moslem.shahverdi@ut.ac.ir, moslem.shahverdi@empa.ch (M. Shahverdi).

https://doi.org/10.1016/j.conbuildmat.2022.126628
Received 2 December 2021; Received in revised form 20 January 2022; Accepted 23 January 2022
Available online 8 February 2022

SMAs have two distinct phases: austenite and martensite. The austenite phase has a symmetric crystalline structure and is typically stable at high temperatures and low stresses. By contrast, the martensite phase has a low-symmetry lattice structure and is typically stable at low temperatures and high stresses [7]. Superelastic behavior is observed in the austenite phase of the SMAs. This property can be exploited to minimize the residual deformations caused by load-induced excitations, such as those originating from earthquake events. By contrast, the SME is exhibited in the martensite phase of the SMAs. In the martensite phase, SMAs experience large residual strains upon unloading. Heating the martensitic lattice structure to a temperature higher than that required to form austenite and then cooling it to room temperature can return the SMA to its initial shape if it is unconstrained (i.e., free to move). However, in the configurations in which the recovery strain is prevented because of external constraints (e.g., clamps and end anchorages), recovery stress is generated in the SMA, which can be utilized for prestressing purposes. The prestressing effects can result in the enhancement of the initial stiffness, crack resistance, and active confinement of the concrete core. Moreover, SMA properties can be employed to incorporate self-centering behavior into RC structures. This behavior refers to the ability of a structural component to regain its original configuration, with minimum residual forces/displacements, after experiencing an extreme loading event.

Among the earliest studies performed to provide an overview of the applications of SMAs in the fields of damping, vibration control, and prestressing of civil structures are the studies of Janke et al. [8] and Song et al. [9]. Subsequently, Ozbulut et al. [10] provided a thorough review of the applications of SMAs as bracing systems, beam-column connectors, isolation devices, and restrainers for seismic response control. More recently, Zareie et al. [6] presented a broad overview of the applications of SMAs as frequency controllers, vibration isolation systems, dampers, and reinforcements in steel, concrete, and timber structures. Despite the variety of reviews on the use of SMAs in structural engineering, the existing literature lacks a holistic review of the current progress, main findings, potential limitations, and prospects of SMA reinforcement (i.e., rebars, strips, wires, and cables) for strengthening and self-centering RC structural elements, such as beams, columns, beam-column joints, and shear walls. In addition, despite the variety of SMAs developed to date, the absence of comprehensive guidance for selecting SMAs with the material properties most suitable for a target application has posed fundamental and practical challenges.

To address such critical gaps, in the current study, we performed a comprehensive review of the experimental studies conducted on the strengthening, repair, and design of RC structural elements (i.e., beams, columns, beam-column joints, and shear walls) using different compositions of SMAs. For this purpose, a thorough survey of the existing literature was performed, covering the period from 2001 to 2020. As shown in Fig. 1 (a), the interest in the investigation of SMAs has been increasing; furthermore, Fig. 1 (b) shows that North America has been leading the research in this critical domain, followed by Europe and Asia. In previous studies, four types of SMAs—Ni-Ti, Ni-Ti-Nb, Cu-Al-Mn, and Fe-Mn-Si—have been mainly considered for civil engineering applications, which are hereafter referred to as Ni-Ti SMA, Ni-Ti-Nb SMA, Cu-SMA, and Fe-SMA, respectively. As shown in Fig. 2 (a), more than half of the past studies have focused on Ni-Ti SMAs, primarily because they are commercially available and used in the automotive, aerospace, robotic, and biomedical industries [11]. However, investigations involving Fe-SMAs for strengthening applications have been growing the fastest from 2016 onwards owing to the superior mechanical properties, low cost, and high machinability of Fe-SMAs compared with those of other SMAs. Fig. 2 (b) shows that approximately half of the available studies were conducted on RC beams, followed by columns, walls, and beam-column joints. The large number of studies focused on beams can be attributed to the ease of application of SMAs to horizontal structural members.

In this review, a brief overview of the key material and mechanical characteristics of SMAs is presented, followed by a description of the installation techniques used for SMAs in strengthening applications. After providing the necessary background, the structural applications of SMAs for beams, columns, beam-column joints, and shear walls are discussed in detail. The studies have been systematically categorized based on the objectives of strengthening/repair, which span self-centering, crack recovery, strength enhancement, confinement, and shear strengthening. This is followed by a comparison section, wherein

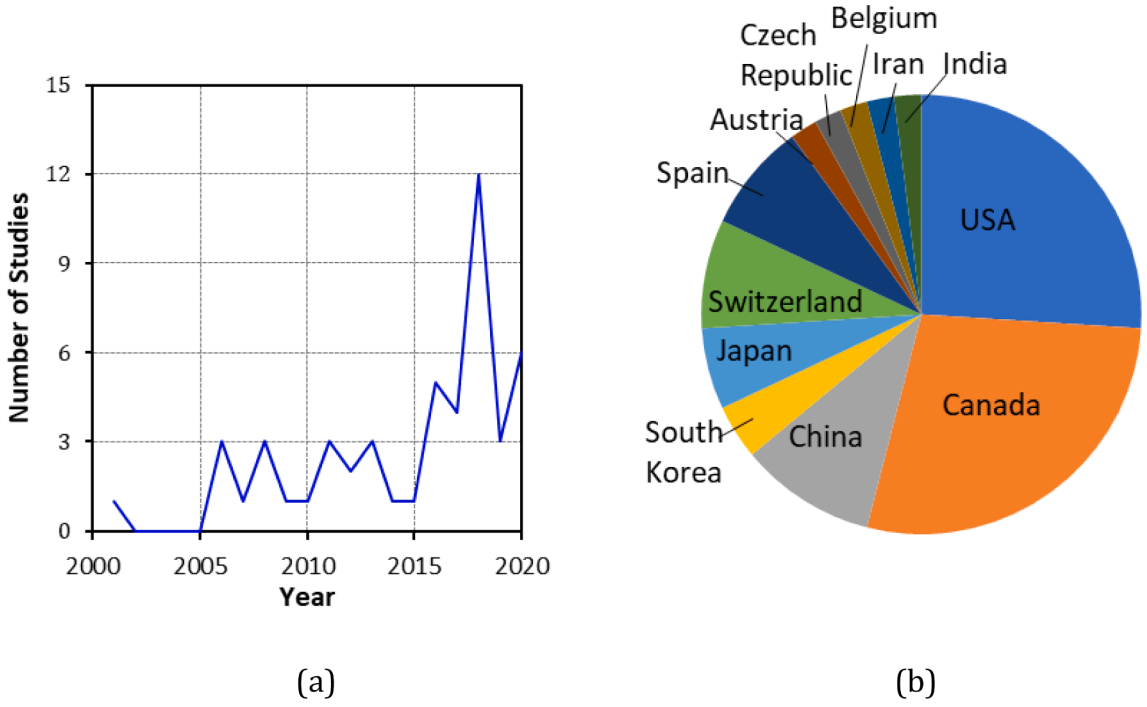

Fig. 1. Distribution of the experimental studies conducted on the strengthening and self-centering of existing and new RC structures with SMAs sorted by (a) year and (b) country.

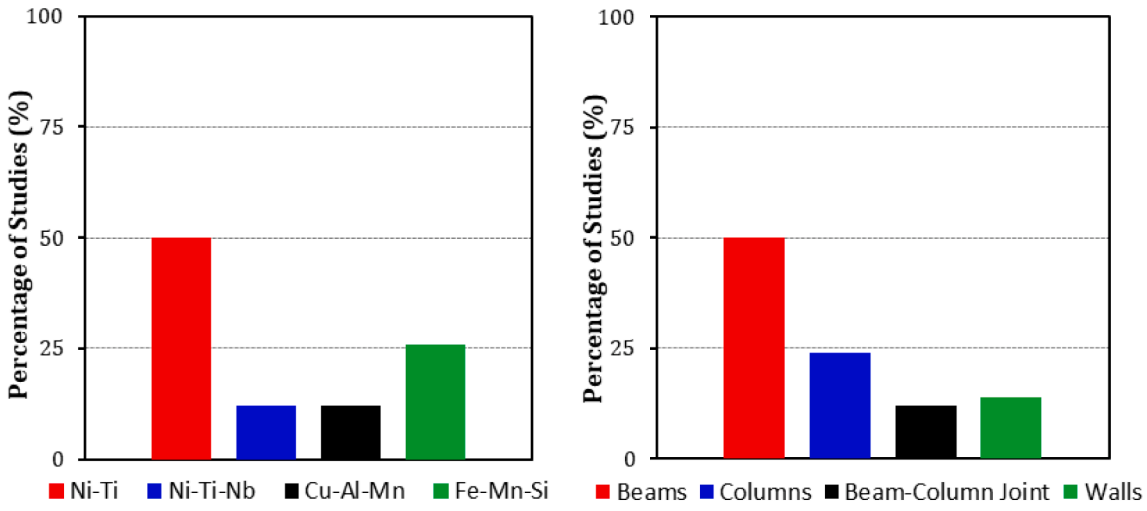

Fig. 2. Distribution of the experimental studies conducted over 2001–2020 on the strengthening and self-centering of existing and new RC structures sorted by the type of (a) SMA and (b) target structural component.

the advantages and disadvantages of strengthening with SMAs are outlined in comparison to conventional strengthening materials and methods. This review concludes with the identification of the challenges associated with using SMAs and future opportunities that can be gained with the proper use of SMAs. The outcome of the current study provides a holistic source of information synthesized in such a way that a wide spectrum of researchers and engineers can directly benefit from the presented details and insights. This will pave the way for future research investigations and practical applications, which can further realize the capabilities of this emerging class of materials.

2. Material and mechanical behavior of SMAs

This section provides an overview of the material, thermomechanical, bond, and long-term behavioral properties of SMAs.

2.1. Material properties

To provide a side-by-side comparison of various SMAs—Ni-Ti, Ni-Ti-Nb, Cu, and Fe-SMA—their key material properties are summarized in Table 1. Ni-Ti SMAs have a high yield stress and a high failure and recovery strain, whereas their elastic modulus is in the intermediate range. Ni-Ti-Nb SMAs have an elastic modulus and yield stress in the low to intermediate range, whereas their failure and recovery strains are in the intermediate to high range. Cu-SMAs have a high recovery strain and a low elastic modulus, yield stress, and failure strain. Finally, Fe-SMAs have a high elastic modulus, yield stress, and failure strain, while their recovery strain falls in the low to intermediate range. The wide range of SMA properties, shown in Table 1, is primarily due to the variety of compositions and treatments (mechanical and thermal) considered for these alloys, depending on the manufacturer and application of interest. Among the four aforenoted SMAs, Ni-Ti SMA and Cu-SMA exhibited excellent superelastic behavior owing to their high recovery strain. This property has been extensively exploited in the available studies for the self-centering of RC structures, where SMAs were included as longitudinal reinforcements in the plastic hinge region. The study of the cyclic behavior of superelastic Ni-Ti SMAs showed that this category of SMAs exhibits a small residual strain (<1%) up to a strain of 6% [12–13]. However, the recentering properties are degraded at cyclic strains greater than 6%. On the other hand, the strain rate has a negligible effect on the recentering behavior of these SMAs. Araki et al. [14] reported that Cu-Al-Mn SMAs exhibit superelastic behavior comparable to that of Ni-Ti SMAs under quasi-static cyclic loads. Ni-Ti-Nb and Fe-SMA, by contrast, exhibit excellent SME, for which the thermomechanical properties are of prime importance.

2.2. Thermomechanical properties

The thermomechanical properties of SMAs, including their activation temperature, recovery stress, and recovery strain, are summarized in Table 1. The efficacy of SME exhibited by SMAs depends on the width of the thermal hysteresis band, activation temperature, and recovery stress. This section provides an overview of the effects of various factors on the SME exhibited by SMAs.

2.2.1. Effect of thermal hysteresis band on recovery stress

The SME is most pronounced in SMAs that have a wide thermal hysteresis between their martensite and austenite phases. The start and

Table 1
Material and mechanical properties of SMAs used for strengthening RC structures.

Type of SMA	Elastic Modulus (GPa)	Yield Stress (MPa)	Failure Strain (%)	Optimum Prestrain (%)	Activation Temperature(^{0}C)	Recovery Stress (MPa)	Recovery Strain (%)
Ni-Ti SMA [8,15–16,18–38]	38–84	379–746	40–50	6–8	100–200	400–700	6–9
Ni-Ti-Nb SMA [16–17,39–42]	25–63	232–350	9–37	6–7	108–200	354–560	5–7
Cu-SMA [7,14,43–47]	20–35	180–210	18	–	–	–	7–12
Fe-SMA [48–62]	75–165	400–550	40	2–4	160–500	130–580	0.15–4.0

finish temperatures of martensite and austenite phases are listed in Table 2 for Ni-Ti, Ni-Ti-Nb, Cu, and Fe-SMA. Notably, the difference between the martensite and austenite start temperatures is greater than 100 °C for Ni-Ti-Nb and Fe-SMA, which makes them suitable for generating large recovery stresses in the order of 130–580 MPa and 354–560 MPa, respectively. In contrast to Ni-Ti-Nb and Fe-SMAs, the difference in the martensite and austenite start temperatures is 15–34 °C for Ni-Ti SMAs and 20 °C for Cu-SMAs. This (relatively) small temperature difference minimizes the potential of Ni-Ti and Cu-SMAs to exhibit a notable SME. Studies conducted on strengthening with Ni-Ti SMAs report the generation of high recovery stresses in the order of 400–700 MPa at activation temperatures of 100–200 °C after the SMAs are prestrained in the range of 5%–8% [15–16]. However, a significant drop in the generated recovery stresses occurs because of short-term relaxation once the heating process is completed and the temperature decreases. This is because the ambient temperature should remain high enough for the SMA to remain in the austenite phase and maintain the recovery stress. However, because the ambient temperature is often close to the martensite phase temperature of Ni-Ti SMAs, they transform back to their martensite phase upon cooling, resulting in the loss of generated recovery stresses [17]. Notably, to effectively use the SME of SMAs for civil engineering applications, the austenite start temperature should be higher than the high ambient temperature (i.e., 40 °C) and the martensite start temperature should be lower than the low ambient temperature (-10 °C) [16].

2.2.2. *Effect of activation temperature on recovery stress*

Generally, the recovery stress is larger at higher activation temperatures. Shahverdi et al. [64] activated a 1.5 mm thick Fe-SMA at temperatures in the range of 120–380 °C and found that the recovery stress increased from 260 MPa to 450 MPa as the activation temperature increased from 120 °C to 380 °C, as shown in Fig. 3. However, higher activation temperatures are not suitable for civil engineering applications as they can adversely affect the bond between concrete and SMA, further to causing the deterioration of the cementitious matrix.

2.2.3. *Effect of prestraining on recovery stress*

The optimum prestrain required for generating the recovery stress is often in the range of 6%–7% and 2%–4% for Ni-Ti-Nb and Fe-SMA, respectively. Choi et al. [65] reported that after stress relaxation, the recovery stress is similar (approximately 200 MPa) for Ni-Ti-Nb SMA prestrained to 3%–7% and heated to 200 °C. In contrast, before stress relaxation, the recovery stress at 7% prestrain is 50 MPa higher than that at 3% prestrain. Similarly, Shahverdi et al. [64] found that the generated recovery stress is similar for prestrain values of 1%–8%, as shown in Fig. 4.

2.2.4. *Effect of cyclic loading on recovery stress*

The activated Fe-SMAs subjected to high cycle-fatigue loads exhibited a negligible decrease in stiffness under cyclic loading. However, a reduction in the recovery stress occurs under cyclic loads, which can be attributed to the reversible phase transformation–induced deformations. At a constant strain amplitude, the reduction in the recovery stress is relatively high during the first cycle, but it decreases with an increase in the number of cycles, as shown in Fig. 5. In contrast, the reduction in the

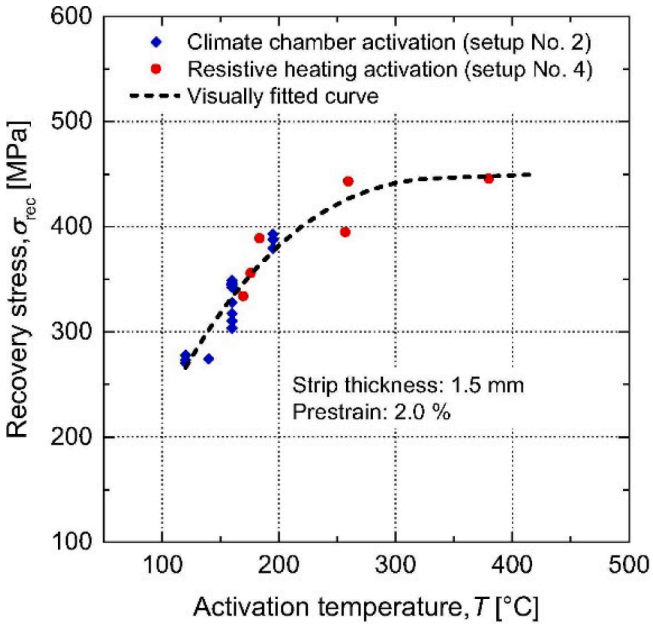

Fig. 3. Effect of activation temperature on the recovery stress of Fe-SMA [64- Elsevier copyright].

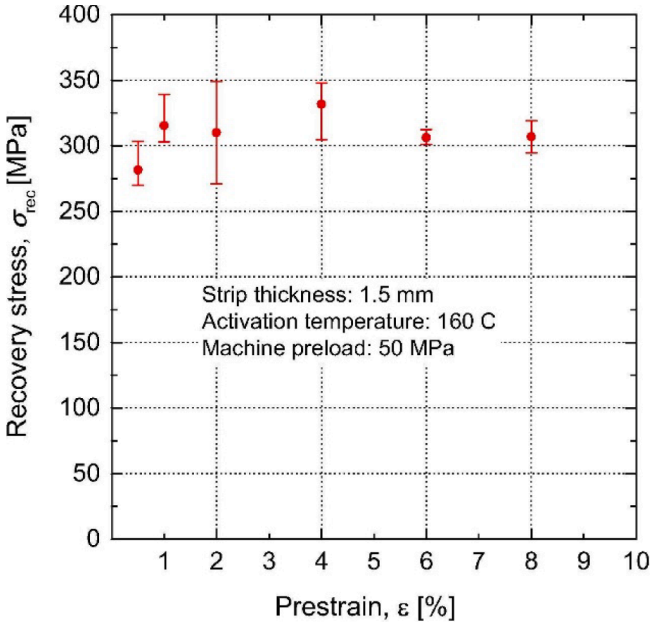

Fig. 4. Effect of prestrain on the recovery stress of Fe-SMA [64- Elsevier copyright].

Table 2
Martensite and austenite start and finish temperatures.

Type of SMA	Martensite's Start TemperatureM_S(^{0}C)	Martensite's Finish TemperatureM_f(^{0}C)	Austenite's Start TemperatureA_s(^{0}C)	Austenite's Finish TemperatureA_f(^{0}C)	Thermal WindowM_s - A_S(^{0}C)
Ni-Ti SMA [18,63]	−5/40	−17/30	10/74	22/82	15–34
Ni-Ti-Nb SMA [16–17,39–40,42]	−105/-18	−135/-74	56/105	74/139	123–161
Cu SMA[45]	−74	−91	−54	−39	20
Fe-SMA[64]	−64	−60	103	163	167

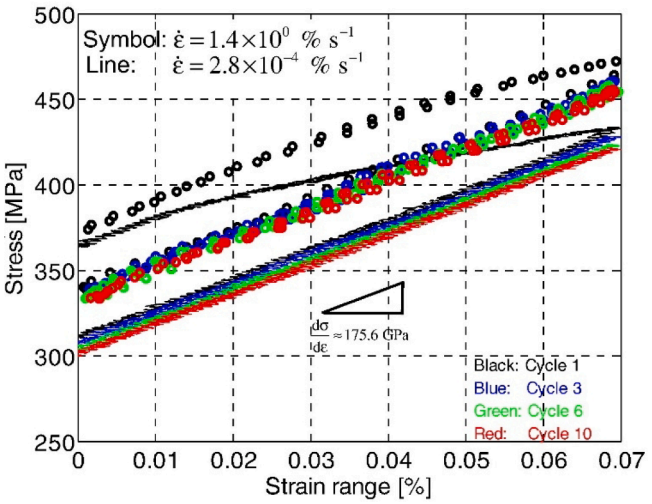

Fig. 5. Recovery stress under of Fe-SMA under cyclic loading [66- Elsevier copyright]

recovery stress increases with increasing strain amplitude. This reduction must be considered in the SMA design and assessment [66]. A reduction in the recovery stress was also reported for activated Ni-Ti-Nb SMAs subjected to cyclic loading. As reported by Choi et al. [65], the recovery stress of Ni-Ti-Nb SMAs can become zero upon unloading from strains equal to or larger than the prestrain applied to them. Hosseini et al. [67] reported that the loss of recovery stress under cyclic loads can be retrieved by a second thermal activation. Investigations on the behavior of non-activated Fe-SMAs under cyclic loads have revealed an asymmetric tension–compression stress–strain behavior, which is both temperature and strain-rate-dependent [68].

2.2.5. *Effect of alloy treatments on recovery stress and superelasticity*

Heat treatment can enhance the recovery stress and superelasticity of SMAs. A recent study [69] showed that at lower aging temperatures (i.e., 600–660 °C), higher recovery and yield stresses can be obtained for Fe-SMA, as compared to those at higher aging temperatures. It was also reported that for a given aging temperature, a higher aging time increases the recovery stress and superelasticity of the material, as shown in Fig. 6. Similar observations were reported upon heat treatment of Ni-Ti-Nb, Ni-Ti, and Cu-SMAs [70–72]. More recently, a study [73] revealed that the additive manufacturing of Fe-SMAs using the laser power bed fusion method can also improve their superelasticity. Notably, while heat treatment can generally improve the properties of as-received SMAs, the elevated temperatures (greater than 200 °C) in the event of a fire during the service life of SMAs can adversely impact their performance [74].

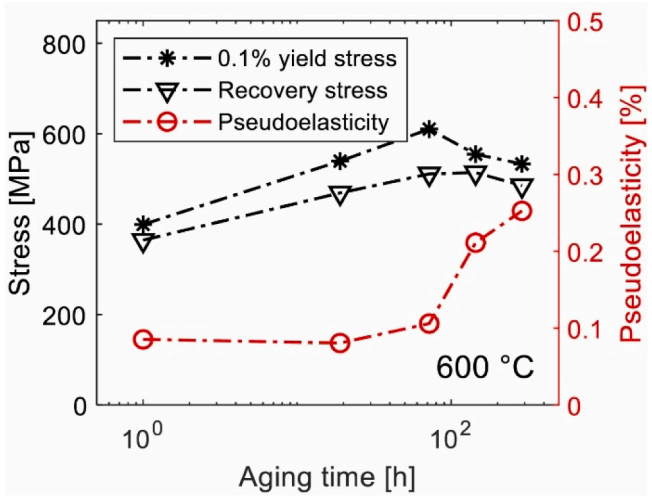

Fig. 6. Effect of thermal ageing on the recovery stress of Fe-SMA [69- Elsevier copyright].

2.3. *Bond behavior*

The bond characteristics of SMAs embedded in concrete govern the required anchorage length, prestress transfer length, and tension-stiffening effects. Previous studies have shown that the bond between concrete and embedded reinforcement can be adversely affected at high temperatures. For instance, pull-out tests conducted on ribbed steel rebars indicated a reduction of 20% and 60% in bond strength at temperatures of 160 °C and 300 °C, respectively [75]. As a potential solution, the bond strength reduction can be limited to 10%–20% if the activation temperature remains below 200 °C [76–78]. Because the minimum temperature required for activating Ni-Ti-Nb and Fe-SMA is below 200 °C, the effect of the activation temperature on the bond behavior is expected to be negligible. This was confirmed by Schranz et al. [79], where no significant difference was observed in the bond strengths of activated (at 160 °C) and non-activated Fe-SMA rebars with full bond lengths in NSM applications. Notably, the reduction in bond strength with increasing temperature also depends on the concrete's compressive strength and the ratio between the concrete cover depth and rebar diameter [80].

Another important factor that can affect bond behavior is the modulus of elasticity of the SMA. Fawaz et al. [75] reported that the bond strength of non-activated Fe-SMA rebars is 15% lower than that of conventional steel rebars, which can also be attributed to the lower elastic modulus of Fe-SMA. This implies that, owing to the relatively low elastic modulus, the rebars made of Ni-Ti, Ni-Ti-Nb, and Cu-Al-Mn SMAs are likely to have a bond strength with concrete not as strong as that which can be achieved with their equivalent Fe-SMA rebars. It is also worth mentioning that while deformed rebars are available for Fe-SMA, the rebars of the other three SMAs are only available in the plain and threaded configurations. Therefore, Daghash and Ozbulut [82] sand-blasted plain Ni-Ti SMA rebars to improve mechanical interlocking to obtain a satisfactory bond performance in NSM applications. However, notably, the low bond strength of SMAs with concrete can be beneficial for certain applications (e.g., self-centering), where the straining and yielding of the rebars are preferred to be delayed. Regarding the anchorage length for the development and transfer of the prestress, Hong et al. [83] recommended using Fe-SMA strips with a minimum length of 600 mm for NSM applications, whereas Fawaz et al. [75] recommended a minimum transfer length of $11d_b$, where d_b is the rebar diameter, for well-confined situations.

2.4. *Long term behavior*

Stress relaxation with time is an important consideration for the long-term behavior of SMAs that exhibit the SME. It has been reported that Fe-SMAs provide a stress relaxation of 10% after 2000 h [64]. Shahverdi et al. [84] monitored the long-term performance of RC beams strengthened with activated Fe-SMA strips in an outdoor exposure environment for four years. The beams were subjected to sustained loads that were higher than their cracking loads. The results indicated a stable prestressing force in the beams as the mid-span deflections remained the same for the beams strengthened with activated and non-activated SMA strips. Stress relaxation in the range of 3%–10% was also reported for Ni-Ti-Nb SMAs, depending on the ambient temperature conditions. However, only minor stress relaxation should be expected within typical variations in ambient temperature [85].

3. Installation techniques for SMAs

SMAs can be implemented in RC structural components using four main techniques: internal reinforcement, NSM reinforcement, embedded reinforcement in a shotcrete layer, and externally fixed reinforcement. Fig. 7 shows a schematic view of each of these four techniques, and this section presents the key details associated with each technique.

3.1. Internal reinforcement system for new RC structural components

SMAs can be used as part of the main internal reinforcement system in new RC structural components, as shown in Fig. 7 (a). In this technique, the steel rebars in the plastic hinge region are replaced with SMA rebars, and the connection between the steel rebars and SMA rebars is then established using mechanical couplers. The main purpose of using SMA rebars as internal reinforcement is to improve the self-centering capacity of RC structural components by exploiting the superelastic behavior of the SMA. In previous studies, only superelastic Ni-Ti and Cu-SMA have been used as internal reinforcements in beams [19,22,43,45,86], columns [7,23–26,41], joints [28–32], and walls [34–38,59]. The SMAs that exhibit a pronounced SME also have the potential to be used as internal reinforcement, mainly as prestressing elements. Most previous studies have concluded that this technique is effective in reducing the residual displacements and minimizing the number and widths of cracks in RC structural components subjected to extreme loading events.

3.2. NSM reinforcement

SMAs can be included as NSM reinforcements in existing RC structures to enhance their flexural strength and introduce the recentering capability after undergoing inelastic displacements. In previous studies, this technique has been primarily used for strengthening RC beams with SMAs [50,52–55,87]. In this method, grooves were first carved in the concrete cover, and SMA rebars were placed in the grooves, which were then filled with an epoxy paste or cement mortar, as shown in Fig. 7 (b). This technique is advantageous, particularly for strength enhancement, crack recovery, and reduction of residual displacements. To date, only one study has utilized this technique for the strengthening of RC columns [27], whereas no study on the NSM strengthening of beam-column joints and walls is available in the literature.

3.3. Embedded reinforcement in shotcrete layer

Embedment of SMA rebars or spirals in a shotcrete layer is another technique that can be used to enhance the flexural strength, improve confinement, and achieve self-centering behavior of the existing RC structural components. To date, the potential of this technique for the strengthening of RC structures with SMAs has only been investigated for RC beams and slabs [15,18,20,51,86,88–89]. In this technique, SMA reinforcement is first fixed to the concrete surface using a mechanical fixation, and then, a shotcrete layer is applied, as shown in Fig. 7 (c). In contrast to other techniques, this technique can be effectively used to introduce a prestressing force to the RC component using the SME of Ni-Ti-Nb and Fe-SMAs.

3.4. Externally anchored reinforcement

SMAs can be externally fixed to the existing RC structural components in the form of wire jackets, spirals, and braces, especially to strengthen them against service and ultimate loads. SMA strips can also be externally anchored to the structural components of interest to enhance their flexural strength, as shown in Fig. 7 (d). In existing studies, this technique has been used for flexural strengthening [48,57] and shear strengthening [21,39,49,56–58] of RC beams, confinement of RC columns [16–17,41–42], and shear strengthening of RC beam-column joints [33] and walls [36,90–91]. This technique often results in enhanced ductility, improved energy dissipation, and reduced residual deformation of strengthened structural components.

A brief overview of the installation techniques provided in this section shows that SMAs can be used as part of the main internal reinforcement system if the objective is to achieve self-centering in new structures using superelastic SMAs. However, the objectives of flexural strengthening and self-centering of existing structures can be effectively achieved by the inclusion of SMAs as NSM reinforcements. Embedment of SMA rebars or spirals in a shotcrete layer is found to be suitable for applications where the SME of the SMA is required to introduce a prestressing force or an active confining pressure for the flexural and/or shear strengthening of RC structural components. Lastly, when SMAs are used as externally anchored reinforcements, both superelasticity and SME can be exploited for strengthening purposes. From the field application perspective, all of the discussed techniques are relatively easy to implement while introducing meaningful advantages compared to conventional strengthening/repair techniques. Among the four techniques developed for the application of SMAs, the inclusion of SMAs as internal reinforcement is the least laborious and the most cost-effective technique as the SMA rebars can be placed during construction, along with other steel rebars. In contrast, the embedment of SMAs in a shotcrete layer would be the most laborious and expensive technique considering labor and equipment requirements. This technique also causes a significant disruption of occupancy compared to other techniques. The techniques involving the use of SMA as NSM or externally anchored reinforcement are moderately laborious, although externally installed SMA reinforcement may not be desired from the perspective of aesthetics. This issue can be resolved through the provision of an aesthetically sound facade in front of the strengthened region.

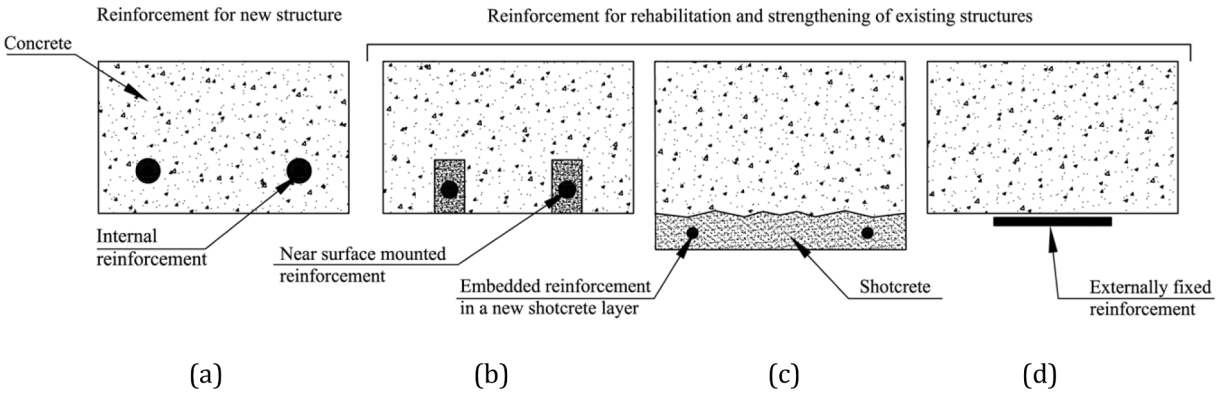

Fig. 7. SMA installation techniques for RC structural components.

4. Structural applications of SMA reinforcement

This section provides a holistic review and systematic discussion of the experimental studies in the literature that utilized SMA reinforcement for RC beams, columns, beam-column joints, and shear walls.

4.1. Beams

RC beams used in buildings and bridges can experience excessive deflections because of structural deterioration and/or increased external loads. Such deflections can lead to cracking and spalling of concrete, questioning the strength and serviceability of RC beams in service. Prestressing the beams using SMAs can effectively control excessive deflections, while flexural and shear strengthening can introduce additional structural capacity using longitudinal and transverse SMA rebars, respectively. The use of superelastic SMAs as internal reinforcements can also help reduce the residual deformations of RC beams under extreme loading events. It is interesting to note that close to half of the existing studies on the application of SMA reinforcement for civil engineering structures focus on RC beams. This is mainly because of the ease of adding SMAs to the horizontal structural members. A summary and the most important contributions of the studies related to the strengthening/repair of RC beams with SMAs are provided in Table 3. The available studies have been categorized based on the purpose of strengthening and the SMA property mainly employed, that is, superelasticity and SME. SMAs are often included in the tension side of RC beams in the form of internal, NSM, embedded, or external reinforcement.

4.1.1. Self-Centering and crack recovery using superelasticity

The superelastic nature of SMA reinforcement makes it appropriate for the self-centering and crack recovery of RC beams. The behavior of RC beams reinforced with superelastic Ni-Ti SMA bars in their critical region, that is, 600 mm of mid-span, as shown in Fig. 8, was investigated by Abdulridha et al. [86] using a four-point bending test setup under monotonic, cyclic, and reversed cyclic loads. Under reversed cyclic loads, the SMA-reinforced specimens recovered 84% of their inelastic mid-span displacements at a displacement ductility of 9.5. The recovery

Table 3
Summary of the studies on RC beams equipped with SMAs (sorted in a chronological order).

Study - Year	Technique	Property Used	Type of Loading	Comparison with Control Specimens			
				Strength	Stiffness	Ductility	Residual Displacement
Soroushian et al. [49] – 2001	Repair using Fe-SMA rods installed externally at cracked regions	SME	Three-point bending	=	↓	=	↓
Deng et al. [18] – 2006	Embedment of Ni-Ti wires in the tension side of the beam	SME	NR	NR	NR	NR	↓
Saiidi et al. [19] – 2007	Ni-Ti rebars as internal longitudinal reinforcement	SE	Four-point bending	↓	↓	↓	↓
Li et al. [15] – 2008	Embedment of Ni-Ti SMA wires followed by jacketing with CFRP plates	SME	Three-point bending	NR	↑	NR	↓
Kuang and Ou [20] – 2008	Embedment of Ni-Ti SMA wires and brittle fibers containing adhesives	SE	Three-point cyclic bending	↓	↓	NR	↓
Abdulridha et al. [86] – 2013	Ni-Ti rebars as top and bottom longitudinal reinforcement at mid-span	SE	Four-point cyclic and reversed bending	↓	↓	↓	↓
Shrestha et al. [43] – 2013	Cu-SMA rebars as top and bottom longitudinal reinforcement at mid-span	SE	Four-point reversed cyclic bending	↓	↓	NR	↓
Pareek et al. [44] – 2014	Cu-SMA rebars as bottom longitudinal reinforcement	SE	Three-point cyclic bending	↓	↓	NR	↓
Shahverdi et al. [50] – 2016	Fe-SMA strips as NSM reinforcement	SME	Four-point bending	↑	↑	↑	NR
Shahverdi et al. [51] – 2016	Fe-SMA rebars embedded in a shotcrete layer	SME	Four-point bending	↑	↑	NR	NR
Mas et al. [21] – 2016	Externally installed Ni-Ti rectangular spirals	SE	Three-point cyclic bending	↑	NR	↑	NR
Rojob and El-Hacha [52] – 2017	NSM Fe-SMA rebars added to the bottom surface	SME	Four-point bending	↑	↑	↑	NR
El-Hacha and Rojob [53] – 2018	NSM Fe-SMA strips at the tension side of the beam	SME	Four-point bending	↑	↑	↓	NR
Rojob and El-Hacha [54] – 2018	NSM Fe-SMA rebars added to the bottom surface	SME	Fatigue loading	↑	↑	=	NR
Pareek et al. [45] – 2018	Cu-SMA rebars as internal longitudinal reinforcement at the beam ends	SE	Cyclic loading	↓	↓	NR	↓
Hong et al. [55] – 2018	Fe-SMA strips as NSM reinforcement	SME	Four-point bending	↑	↑	=	↓
Michels et al. [48] – 2018	Externally anchored Fe-SMA strips to the tension side of the beam	SME	Four-point bending	↑	↑	NR	NR
Montoya-Coronado et al. [56] – 2018	Externally installed Fe-SMA strips as spirals	SME	Three-point bending	↑	↑	↑	NR
Strieder et al. [57] – 2018	Externally anchored Fe-SMA strips to the tension side of the beam	SME	Four-point bending	↑	↑	NR	NR
Rius et al. [39] – 2019	Externally installed Ni-Ti-Nb wires as spirals	SME	Four-point bending	↑	↑	↑	NR
Sinha et al. [40] – 2020	Repair using NSM Ni-Ti-Nb wires at the tension side of the beam	SME	Four-point cyclic bending	↑	↑	NR	↓
Cladera et al. [58] – 2020	Externally installed Fe-Mn Strips as spirals	SME	Three-point bending	↑	↑	NR	NR
Azadpour and Maghsoudi [22] – 2020	Ni-Ti strands as internal longitudinal reinforcement at the top and bottom of the beam	SE	Cyclic bending	↑	=	↑	↓
Czaderski et al. [96] – 2021	Fe-SMA stirrups as embedded reinforcement	SME	Four-point bending	↑	↑	↑	NR

Notations: SE, superelasticity; SME, shape memory effect; NR, not reported; ↑, increased; ↓, decreased; =, same.

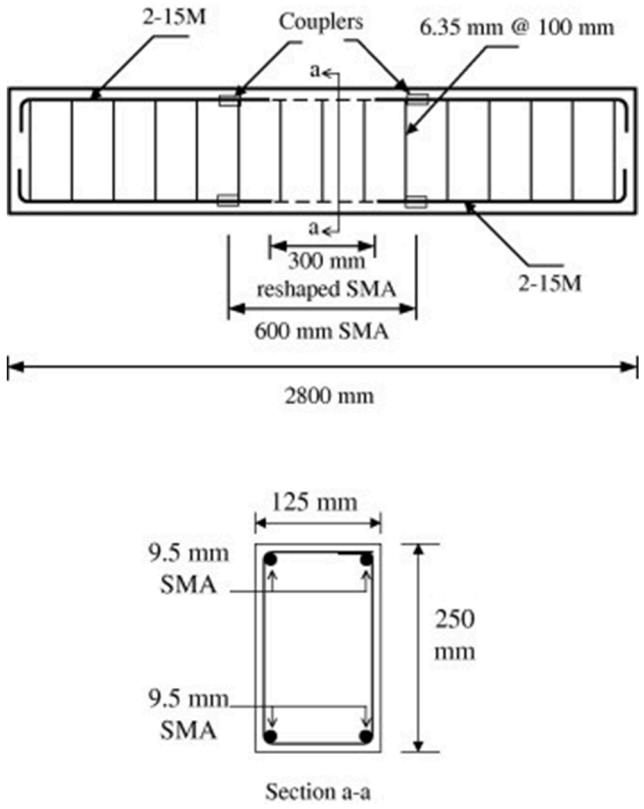

Fig. 8. Installation of superelastic Ni-Ti SMA in the mid-span [86-Elsevier copyrights].

of the inelastic displacements, however, did not exceed 26% in the conventional RC beams of the same size tested in parallel. In addition, the strength and ductility of the SMA-reinforced beams were comparable to those of conventionally designed specimens. However, the energy dissipation of the SMA-reinforced beams under reversed cyclic loads was 54% of that of conventional RC beams. This was attributed to the flag-shaped hysteretic behavior of the superelastic SMAs.

The feasibility of using superelastic Cu-SMA rebars as a partial replacement for steel rebars in the mid-span region was evaluated by Shrestha et al. [43], as shown in Fig. 9. This was with the immediate goal of reducing cracks formed in concrete beams under cyclic loads. The results of this experimental study showed the superior self-centering and crack recovery capabilities of SMA-reinforced beams (with or without pre-tensioning). As such, a crack width recovery of 4.7 mm and 4.3 mm was observed upon unloading the SMA-reinforced beams with and without pre-tensioning, respectively. This was a significant improvement compared to the crack width recovery of 0.5 mm recorded in the conventional RC beams tested in the same study.

Pareek et al. [44] evaluated the effectiveness of an externally activated self-repairing technique, based on superelastic Cu-SMA reinforcing rebars, in conjunction with an epoxy injection network. For this purpose, beams with reinforcement alternatives of deformed steel rebars, threaded steel rebars, and threaded SMA rebars were considered. It was reported that the specimen with the threaded SMA rebars successfully exhibited a flag-shaped hysteresis loop with a relatively large displacement recovery. However, the specimens with deformed and threaded steel rebars exhibited large residual deformations. The residual crack width was also observed to be the smallest for the SMA-reinforced beam. The relocation of the plastic hinge region after using superelastic Cu-SMA rebars was also studied by Pareek et al. [45]. Four beams were considered in the cited study, in which steel rebars were provided in the first beam, and a combination of steel and SMA rebars was included in the other three beams, as shown in Fig. 10. To move the plastic hinge region along the beam length, the longitudinal centroids of the SMA rebars were positioned at the end, 0.5D from the end, and 1D from the end of the beam, where D is the depth of the beam. The beams were tested such that the maximum moments were at the beam ends, while the mid-span experienced no bending moment. The experimental test results showed that the plastic hinge can be designed to coincide with the location of the SMA rebars owing to their (relatively) low yield stress. This introduces the possibility of moving the plastic-hinge region away from the beam end. It must be noted that the inclusion of SMA rebars at the location of the maximum moment can result in lower strength and energy dissipation in RC beams because of the low yield stress/elastic modulus of SMAs compared to that of steel. However, with the relocation of the plastic hinge, the drawbacks associated with strength and energy dissipation were found to be addressed to a great extent.

In a study conducted by Azadpour and Maghsoudi [22], superelastic Ni-Ti SMA strands were employed to strengthen continuous normal and high-strength RC beams. The SMA strands were provided in the critical

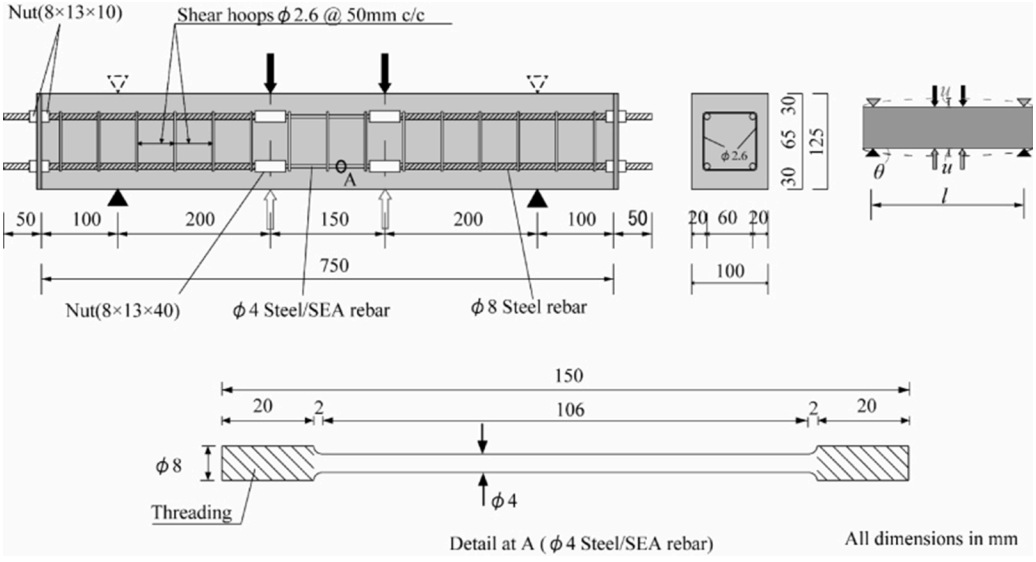

Fig. 9. Superelastic Cu-SMA used in the mid-span of the beam, where attachment to the steel reinforcement was achieved using a set of couplers [43-IOP Publishing Ltd Copyrights].

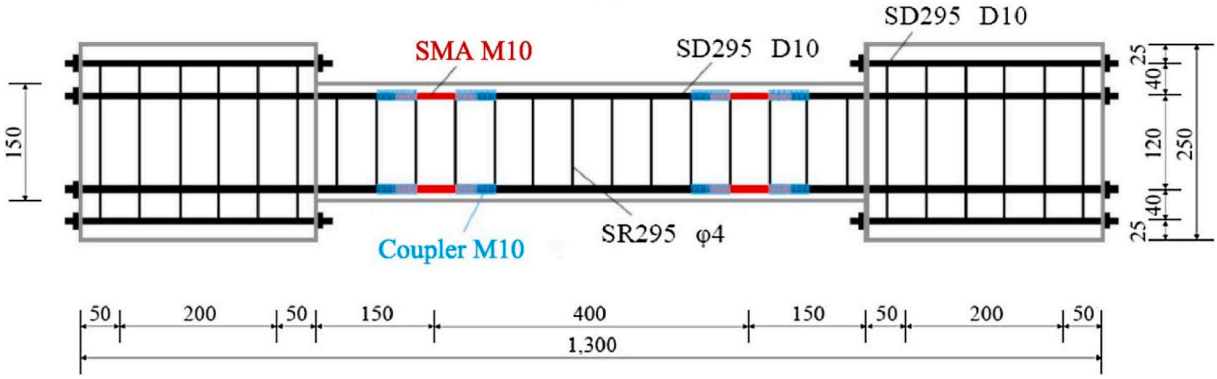

Fig. 10. Superelastic SMA and steel rebars incorporated into the RC beam [45-Elsevier Copyrights].

sagging and hogging regions of the beams. It was reported that high-strength RC beams reinforced with SMA strands displayed superior performance in recovering flexural cracks because SMAs exhibited better superelasticity in high-strength beams. In contrast, normal-strength RC beams exhibited a high potential to recover mid-span deflections in comparison to high-strength concrete beams, which can be attributed to the brittle nature of high-strength concrete. The results showed that up to 90% of the mid-span deflection was recovered in the SMA-reinforced beams, alongwith a 50% increase in the energy absorption capacity, in comparison to conventional beams of the same size. The cited study concluded that the performance of high-strength RC beams could be further improved if the size of SMA strands was increased.

Kuang and Ou [20] proposed a self-repairing concrete beam equipped with superelastic Ni-Ti SMA wires, in conjunction with adhesives included in a set of hollow fibers that ran throughout the length of the beam (Fig. 11). The main premise of the technique was that, at large deformations, the brittle fibers would rupture and adhesives would be released to fill up and close the cracks once the SMA wires recover the deflections of the beam with their superelasticity. The experimental tests showed that, upon unloading after large deformations (up to 2% of the span length), the mid-span deflection of the SMA-reinforced beam was reversed, and the cracks were almost entirely closed.

In a pilot study, Saiidi et al. [19] compared the responses of four small-scale concrete beams reinforced externally at the mid-section with superelastic Ni-Ti SMA bars to that of four conventional steel-reinforced beams under four-point bending tests. The reinforcement ratio at the mid-span was the main variable explored in this study. The experimental test results showed that the residual displacements in the SMA-reinforced beams were 1/5th of the residual displacements in steel-reinforced beams of the same size. However, the stiffness of the SMA-reinforced beams was 60% lower than that of steel-reinforced beams owing to the lower modulus of elasticity of Ni-Ti bars compared to steel bars. The study concluded that a combination of high-strength steel and Ni-Ti rebars can result in RC structural components that benefit from adequate stiffness while offering the ability to partially recover deformations. In a separate effort, Mas et al. [92] demonstrated the application of superelastic Ni-Ti cables as longitudinal reinforcements in concrete beams. The experimental test results showed that the beams reinforced with Ni-Ti cables exhibited a significantly lower stiffness than steel-reinforced beams, mainly because of the low modulus of elasticity of the Ni-Ti SMA. The cited study concluded that an increase in the modulus of elasticity of Ni-Ti cables may reveal promising avenues for their application in structural engineering. Other studies have investigated the feasibility of using Ni-Ti SMA cables as restrainers for concrete girders [93] and as self-centering braces for steel structures [94–95].

From the synthesis of the studies performed on RC beams, we can infer that the residual displacements in the beams reinforced with superelastic SMAs are 10–20% of the residual displacements observed in conventional steel-reinforced concrete beams. This makes the superelastic SMA reinforcement promising for incorporating self-centering behavior into RC beams. However, SMA-reinforced beams generally show an initial stiffness and strength lower than those of their steel-reinforced counterparts mainly because of the lower elastic modulus and yield strength of SMAs than those of steel materials. Similarly, the energy dissipation of SMA-reinforced beams under cyclic loads is lower than that of conventional RC beams because of their flag-shaped hysteresis loops. A variety of superelastic SMA reinforcement ratios, ranging from 0.12% to 2.10%, have been used in previous studies. However, no recommendation has been made regarding the optimum amount of SMA reinforcement required for the satisfactory self-centering of RC beams. The findings of previous studies also show that the capabilities of SMAs can be further improved if they are paired with high-strength steel and/or fiber/adhesive systems.

4.1.2. *Strength enhancement and self-centering using shape memory effect*

The SME exhibited by SMAs has been extensively used to prestress RC beams. The activation of SMA rebars results in large recovery stresses, which help improve the structural performance of RC beams by

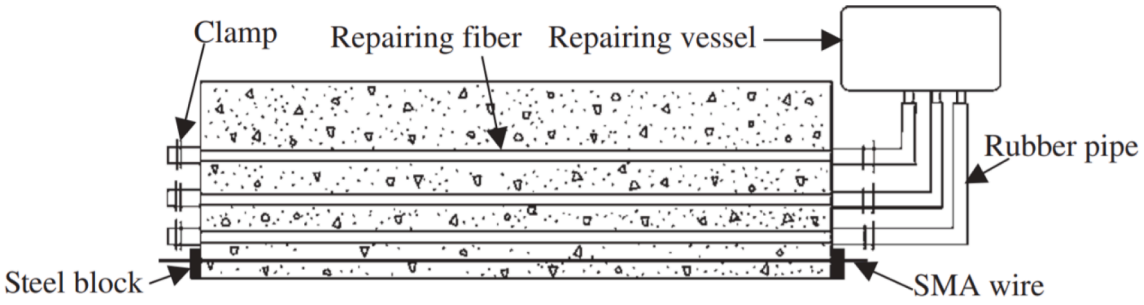

Fig. 11. Schematics of the self-repairing concrete beam fabricated with embedded SMA wires, along with fibers containing adhesives [20-IOP Publishing Ltd Copyright].

enhancing their strength and reducing the risk of experiencing cracks. Moreover, SME helps increase the initial stiffness of the beams and improves their self-centering behavior. To exploit the SME for flexural strengthening purposes, SMAs are commonly provided as NSM, embedded, or external reinforcements. Among the past studies, Deng et al. [18] evaluated the performance of embedded Ni-Ti SMA wires in controlling the deflection of RC beams. They reported that a large recovery force was generated upon the thermal activation of the embedded SMA wires, which reversed the deflection of the tested beam from downward to upward. Furthermore, an increase in the prestrain of the SMA wires from 6.0% to 8.0% improved the recovery force. In addition, the recovery force increased with an increase in the number of SMA wires. It was determined that, with the same total cross-sectional area of the embedded SMA wires, the small-diameter SMA wires resulted in a better deflection control than the large-diameter SMA wires.

To improve the seismic behavior of RC beams, Li et al. [15] used SMA wires in combination with carbon-fiber-reinforced polymer (CFRP) plates. It has been reported that the thermal activation of Ni-Ti SMA wires significantly reduces the residual deformation and cracking potential of the beams. In addition, with an increase in the number and embedment length of the SMA wires, the reduction in the residual deformation became more pronounced. The provision of CFRP plates in addition to SMA wires increased the stiffness and reduced the damage observed in the tested specimens. The cited study concluded that temporary strengthening by SMA wires followed by permanent strengthening by CFRP plates can be an effective method to strengthen RC structures. The application of NSM Fe-SMA strips for the flexural strengthening of RC beams was studied by Shahverdi et al. [50]. The experimental procedure comprised four steps: prestraining of the strips up to 1.5%, grouting of the strips into grooves, activation of the strips by resistive heating and cooling, and finally, loading of the strengthened beams until failure under a four-point bending test. Fig. 12 shows the embedment of the strips into the grooves and the setup used for thermal activation of the SMA strips. The cracking load for specimens with activated SMA strips was 80% higher than that for specimens with non-activated SMA strips. A significant reduction in the mid-span vertical deflection was also reported for beams with activated SMA strips. The recovery stresses generated were up to 200 MPa, and a satisfactory bond behavior was observed between the cement mortar and SMA strips placed in the grooves.

In a separate study, Shahverdi et al. [51] evaluated the viability of RC beams strengthened by ribbed Fe-SMA rebars embedded in a shotcrete layer, as shown in Fig. 13. The beam with the ribbed SMA rebars exhibited an approximately two times higher cracking load resistance compared to the beam with ribbed steel rebars. At a mid-span deflection of 0.2%, the loads resisted by the beams strengthened with two- and four-ribbed SMA rebars were 163% and 265% higher than those resisted by the unrepaired beam, respectively. The cited study revealed recovery stresses of up to 300 MPa for the Fe-SMA rebars upon activation at 160 °C. The study noted that the development of shrinkage cracks in the shotcrete layer can be a potential issue associated with this strengthening technique, which requires further investigation.

Michels et al. [48] mechanically anchored Fe-SMA strips to the tension side of RC beams for flexural strengthening. The strips were prestrained to 2% and activated by resistive heating at 160 °C. The experimental test results showed a significant enhancement in the flexural strength of the beams strengthened by the Fe-SMA strip in comparison to the conventional beams and beams strengthened by CFRP strips. Moreover, the Fe-SMA strip-strengthened beams exhibited enhanced stiffness, which lowered the vertical deflection experienced in the four-point bending tests. Rojob and El-Hacha [52] also employed NSM Fe-SMA rebars for prestressing RC beams. The SMA rebars were grooved into the tension side of the RC beams with an initial prestrain of 6% and then activated at temperatures above 300 °C. An increase of more than 30% was reported in the yield and ultimate load-bearing capacity, as well as the ductility of the RC beams after prestressing. The cited study concluded that SMA strengthening can be superior to FRP strengthening because it leads to an increase in both strength and ductility, as opposed to FRP strengthening, in which a strength-ductility tradeoff is often observed. In another paper, El-Hacha and Rojob [53] proposed NSM Fe-SMA strips to be used at the tension side of RC beams for flexural strengthening. The SMA strips were prestrained to 3% and then activated by heating above 150 °C. The test results demonstrated an increase of 30%–60% in the flexural strength of the beams strengthened with activated SMAs compared to the unrepaired control specimen. Furthermore, the ductility of the strengthened beams was comparable to that of the control specimen. The comparison of NSM Fe-SMA-strengthened beams with NSM CFRP-strengthened beams revealed that the latter exhibited a slightly higher strength but significantly lower ductility than the former.

The performance of RC beams with NSM Fe-SMAs was investigated under fatigue loads by Rojob and El-Hacha [54]. The strengthened beams performed better than the control beam at low levels of fatigue load (corresponding to the lower and upper limits of the stress level in the tension reinforcement of the beam, i.e., 0.29 f_y and 0.53 f_y , respectively). However, at high levels of fatigue load (corresponding to the lower and upper limit of the stress level in the tension reinforcement of the beam, i.e., 0.45 f_y and 0.68 f_y , respectively), the bond between the SMA rebar and the grouting material started degrading. The continued degradation resulted in high stress levels at the anchors, leading to the rupture of the SMA rebars at the location of the anchors after 5.5 million load cycles. In another study, Hong et al. [55] investigated the flexural behavior of RC beams strengthened with NSM strips of Fe-SMA. The SMA strips were embedded in the grooves carved into the concrete cover and then bonded to the concrete substrate using rapid-hardening cement, as shown in Fig. 14. The strips were then activated by

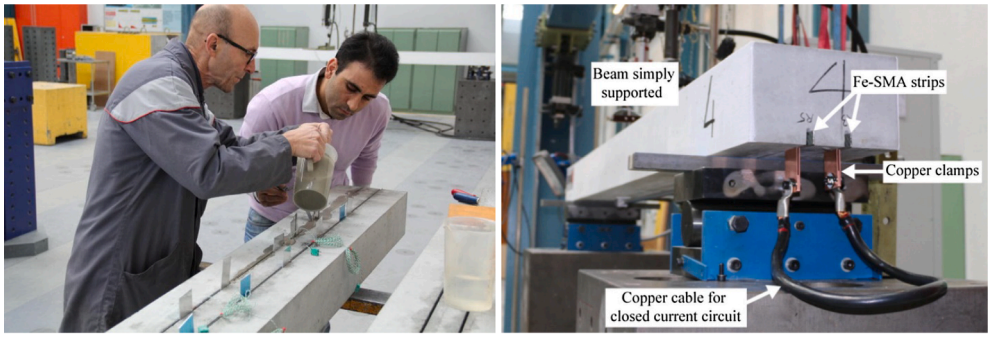

Fig. 12. Flexural strengthening of an RC beam with Fe-SMA strips: (a) embedding the Fe-SMA strips into the grooves formed in the concrete cover using a cement-based grout and (b) setup for the activation of SMA strips using a resistive heating procedure [50-Elsevier Copyrights].

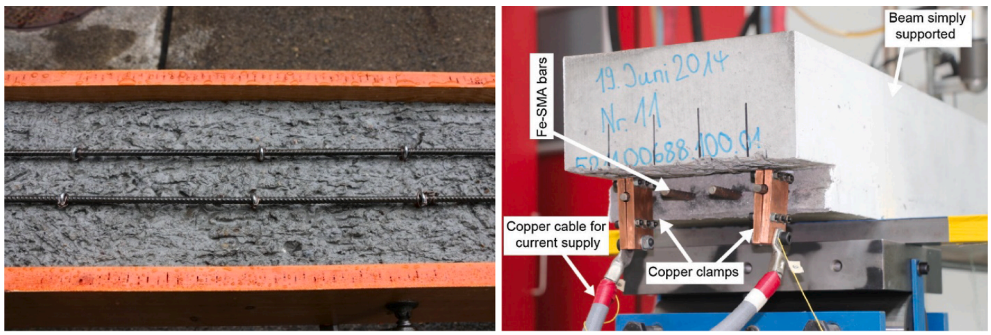

(a) (b)

Fig. 13. Flexural strengthening of an RC beam with Fe-SMA rebars: (a) ribbed SMA rebars fixed on the old concrete (after surface preparation) and (b) beam with the SMA rebars after shotcreting [51-Elsevier Copyright].

(a) (b)

Fig. 14. Installation of NSM Fe-SMA strips: (a) strips connected with copper clips for electric resistive heating and (b) the process of filling the grooves with cement mortar [55-Springer Copyright]

electrical resistive heating at 160 °C. The recovery stress of the activated strips induced a compression force in the tension region of the beams, which resulted in a cambering effect at the mid-span. The cracking loads resisted by the beams with the SMAs activated with a prestrain of 2.0% and 4.0% increased by 16% and 35%, respectively, compared to those of the specimens with non-activated SMAs. A notable increase in the ultimate load-carrying capacity of the specimens was also reported, which increased further with an increase in the number of SMA strips. In addition, the prestressing effect did not decrease the ductility of the tested specimens, in contrast to the prestressed FRP systems.

Strieder et al. [57] used thermally activated Fe-SMA strips for external tensile strengthening of RC beams in flexure. The ultimate load of the SMA-strengthened beams increased by 160% compared to that of the reference beams. In addition, the cracking load of the strengthened beams increased by more than three times. The cited study revealed that the performance of RC beams can be further improved by a second thermal activation. The repair of damaged RC girders using thermally activated NSM Ni-Ti-Nb SMA wires was experimentally studied by Sinha et al. [40]. SMA wires were installed in the grooves carved in the bottom cover of the cracked girder and then anchored at both ends. The wires were prestrained to 2.5% and thermally activated at 150 °C. This repair technique was found to reduce the crack widths by 74% while recovering the residual mid-span deflection by up to half. Increases of 31% and 45% were also observed in the cracked stiffness and ultimate moment capacity of the tested girders, respectively.

The studies reviewed in this section indicate that the SME of SMAs can be effectively utilized to enhance the strength and initial stiffness of RC beams. For example, a 0.14% reinforcement ratio of activated SMA was found to increase the cracked stiffness of the beam by 31% [40]. Similarly, depending on the type of strengthening technique used and the amount of SMA reinforcement provided, an increase of up to 265% can be observed in the load-carrying capacity of the beams strengthened with activated SMA reinforcement. The SME provided by the SMA reinforcement also reduced the mid-span deflections and residual displacements of the beams under monotonic and cyclic loads. Notably, the outlined improvements in structural performance were achieved with SMA reinforcement ratios in the range of 0.1%–0.5%. The experimental test results indicate that the embedment of SMAs in a shotcrete layer is more appropriate for strength and stiffness enhancement applications as the largest increase in the load-carrying capacity was observed for beams with SMA reinforcement embedded in a shotcrete layer. While the three installation techniques (i.e., NSM, embedded, and external reinforcement) were reported to be suitable for reducing residual deformations, further investigations are required to determine the most effective installation technique(s).

4.1.3. *Shear strengthening*

SMAs can be used in the form of internal spirals or external wire jackets/braces for shear strengthening of RC beams. The only study conducted to exploit the superelastic behavior of SMAs for shear strengthening was that by Mas et al. [21], who investigated the effect of superelastic Ni-Ti SMA rectangular spirals (shown in Fig. 15) on the ductility of shear-critical RC beams. The experimental test results showed that Ni-Ti SMA spirals improved the ductility and led to large crack widths at the point of failure, as opposed to conventional RC beams. In addition, the Ni-Ti SMA spiral reinforced beams sustained a significant shear force even at large deflections, whereas a sudden drop in the load carrying capacity was observed in the conventional RC beams of the same size after the development of the critical shear crack.

The recovery stresses generated by the SME can also be useful for strengthening beams with shear deficiency. The earliest study investigating the effectiveness of Fe-SMA rods for the repair and strengthening of damaged RC beams was conducted by Soroushian et al. [49]. They designed an RC beam to be shear-deficient at the cut-off location of the longitudinal bars and subjected it to three-point bending. The damaged beam was then repaired with diagonal SMA rods installed externally at the bar cut-off location. The SMA rods were prestrained to 3% and then activated at 300 °C. The repaired beam was then loaded to failure. The results showed that the original load-carrying capacity of the beam was restored by more than 90% after the repair. The developed technique was then utilized to repair cracked T-beams of a bridge structure. It was reported that the crack width of the T-beams was reduced by 40% upon post-tensioning with SMA rods. In a separate study, Rius et al. [39] used Ni-Ti-Nb SMA spiral wires for shear strengthening of RC beams. The SMA spirals were wrapped around the beam specimens and then activated at 200 °C. The retrofitted beams exhibited an overall ductile behavior, further to a significant increase in their shear strength. The results showed that the pre-cracked beams that were loaded to 98% of their shear capacity and later retrofitted with SMA spirals performed similarly to the specimens that were retrofitted before cracking. The cited study concluded that the retrofitting of the beams with Ni-Ti-Nb

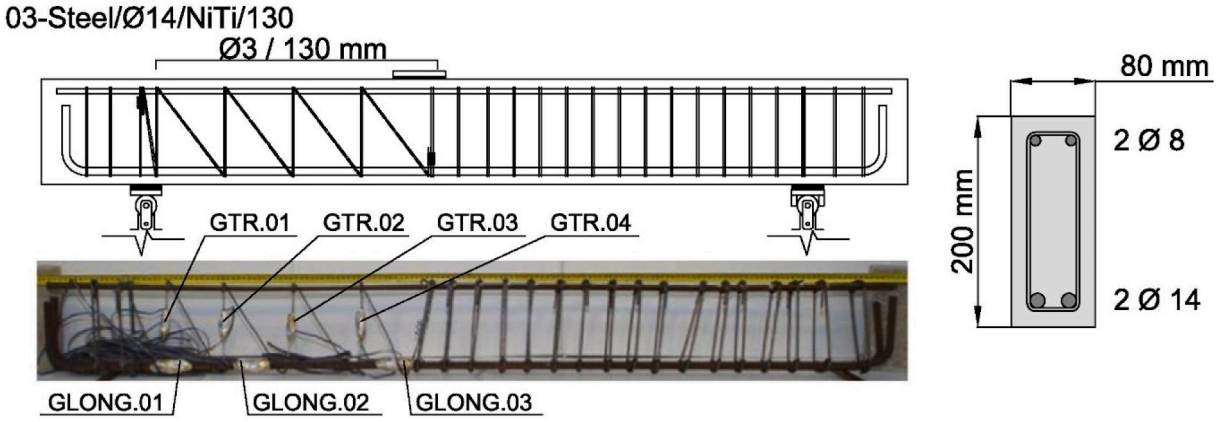

Fig. 15. Shear strengthening of a RC beam with Ni-Ti spirals (Symbol "G" refers to the location of strain gauges) [21-Elsevier Copyrights].

SMA spirals is promising, despite some losses in recovery stresses due to geometric imperfections.

Montoya-Coronado et al. [56] explored the shear strengthening of deficient RC beams using Fe-SMA strips. For this purpose, a set of RC beams was externally wrapped with prestrained Fe-SMA strips thermally activated at 160 °C. A significant increase was reported for the shear strength (up to more than 80%), leading to flexural failure of the strengthened beams, in contrast to the unstrengthened beams that failed in shear. Improved ductility was also recorded for the strengthened specimens, confirming the effectiveness of the proposed strengthening technique. Similarly, Cladera et al. [58] proposed the shear strengthening of RC T-beams using U-shaped Fe-SMA strips externally anchored to the T-beam web, as shown in Fig. 16. The strips were first prestrained and thermally activated at 160 °C. The experimental test results demonstrated a 30% increase in the shear capacity of the strengthened beams compared to that of the reference beam. The appearance of cracks in the strengthened beams was delayed, and the crack width was reduced. However, the ductility of the specimens was less than expected, which was attributed to the method of anchoring of the SMA strips to the web of the T-beam.

More recently, Czaderski et al. [96] utilized both activated and non-activated Fe-SMA stirrups embedded in a mortar layer for shear strengthening of large-scale T-beams. The U-shaped stirrups were first installed in holes drilled inside the flange, and then, a mortar layer was sprayed to embed the stirrups, as shown in Fig. 17. The activated SMA stirrups resulted in a greater reduction in the beam deflection, number and width of cracks, and stresses in the internal steel at the serviceability limit state, in contrast to non-activated stirrups. In addition, a significant enhancement in the shear capacity of the beams was observed. As such, an increase of 71% and 86% was observed in the load-carrying capacity of the strengthened beams for SMA stirrup reinforcement ratios of 0.31% and 0.47%, respectively. The applied load at which the shear cracks developed was found to be higher for the beams with activated Fe-SMA stirrups than for those with a similar amount of non-activated Fe-SMA stirrups. The cited study stated that the proposed strengthening technique is well-suited for onsite applications owing to its ease of application.

From the synthesis of the findings and observations available in the literature, we can infer that the SME of SMAs is useful for shear strengthening applications because of the active confining pressure exerted on the core of the beam, which enhances both strength and ductility properties. The SMA stirrup reinforcement ratios of 0.18%–0.47% used in previous studies increased the shear strength of the beam in the range of 30%–86%. The experimental test results showed that Fe-SMA stirrups employed in the form of ribbed bars resulted in a greater enhancement of shear strength compared to jacketing with Fe-SMA strips. This is primarily because the stirrups were embedded in an additional layer of mortar in the beam web. Therefore, the enhancement in shear strength, in this case, is due to the combined action of stirrups and the additional layer of mortar, whereas the enhancement of shear strength in the case of jacketing with Fe-SMA strips can be solely attributed to the confinement provided by SMA strips.

4.2. Columns

Columns are the main vertical load-carrying components of RC buildings and bridges. As such, the collapse of a single column can trigger a progressive collapse of the entire structure. Deficient RC columns usually need to be strengthened either to upgrade their flexural strength or to improve their confinement to resist lateral loads. SMAs can be useful for strengthening RC columns owing to their superelasticity and SME. Superelastic SMAs can be used to add self-centering behavior to RC columns. In contrast, the SME can be exploited to prestress RC columns, instead of using conventional prestressing techniques, which often introduce practical difficulties. A holistic summary of the existing studies that utilized SMAs for strengthening RC columns

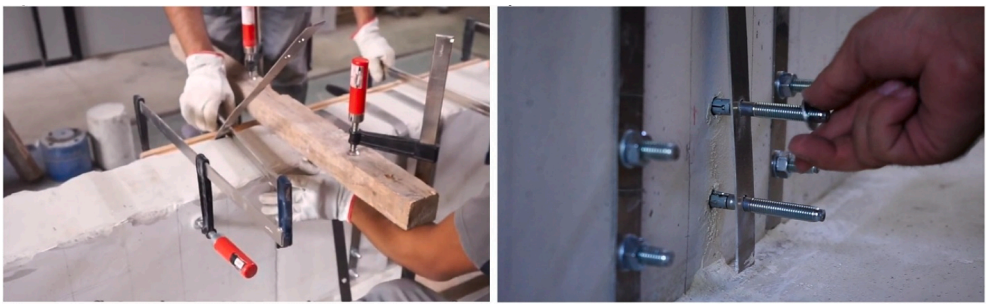

Fig. 16. Shear strengthening of a T-beam with Fe-SMA strips: (a) prestrained strips placed on the beam web and (b) anchorage using mechanical fastners [58-Elsevier Copyright].

(a) (b)

Fig. 17. Shear strengthening of a T-beam with Fe-SMA stirrups: (a) installation of Fe-SMA stirrups and (b) application of spray mortar for embedding the stirrups [96-Elsevier Copyright].

Table 4
Summary of studies on the RC columns equipped with SMAs (sorted in chronological order).

Study - Year	Technique	Property Used	Type of Loading	Comparison with Control Specimens			
				Strength	Stiffness	Ductility	Residual Displacement
Saiidi and Wang [23] – 2006	Ni-Ti SMA rods as internal longitudinal reinforcement with ECC in the plastic hinge	SE	Dynamic loading using shake table	↑	NR	↑	↓
Saiidi et al. [24] – 2009	Ni-Ti SMA rods as internal longitudinal reinforcement with ECC in the plastic hinge	SE	Quasi-static reversed cyclic loading	↓	↓	↑	↓
Shin and Andrawes [17] – 2011a	Ni-Ti-Nb SMA as external spirals	SME	Quasi-static reversed cyclic loading	↑	NR	↑	NR
Shin and Andrawes [41] – 2011b	Repair through the provision of Ni-Ti-Nb SMA as external spirals	SME	Quasi-static reversed cyclic loading	=	↑	↑	NR
Noguez and Saiidi [25] – 2012	Ni-Ti SMA rods as internal longitudinal reinforcement with ECC in the plastic hinge	SE	Dynamic loading using shake table	NR	NR	↑	↓
Choi et al. [16] – 2012	Ni-Ti and Ni-Ti-Nb SMA external wire jackets in the plastic hinge	SME	Quasi-static reversed cyclic loading	↑	=	↑	NR
Hosseini et al. [7] – 2015	Cu-SMA rods as internal longitudinal reinforcement in the plastic hinge along with an ECC tube	SE	Quasi-static reversed cyclic loading	↓	↓	NR	↓
Tazarv and Saiidi [26] – 2016	Ni-Ti SMA internal rods in the connection or plastic hinge	SE	Quasi-static reversed cyclic loading	↑	↓	↑	↓
Varela and Saiidi [97] – 2016	Ni-Ti SMA internal rods in a plastic hinge element made of rubber attached to a concrete-filled CFRP tube	SE	Dynamic loading using shake table	NR	NR	NR	↓
Varela and Saiidi [46] – 2017	Ni-Ti and Cu-SMA rods as internal longitudinal reinforcement in a plastic hinge strengthened with ECC	SE	Dynamic loading using shake table	NR	NR	NR	↓
Jung et al. [42] – 2018	Retrofit and repair using Ni-Ti-Nb SMA spirals	SME	Bidirectional dynamic loading using shake table	↑	NR	↑	↓
Xing et al. [27] –2020	Ni-Ti SMA rods as NSM reinforcement along with CFRP jacket	SE	Quasi-static reversed cyclic loading	↑	=	↑	NR

Notations: SE, superelasticity; SME, shape memory effect; NR, not reported; ↑, increased; ↓, decreased; =, same

is presented in Table 4. Studies have been categorized based on the purpose of strengthening, that is, self-centering, strength enhancement, and/or confinement improvement, as well as the SMA property primarily utilized, that is, superelasticity and/or SME.

4.2.1. Self-Centering and strength enhancement using superelasticity

Superelastic SMAs are mostly provided as internal reinforcements in the plastic hinge region of the columns to achieve self-centering behavior. The first exploratory study to assess the contribution of Ni-Ti SMAs in reducing the residual displacements of RC columns under earthquake excitations was conducted by Saiidi and Wang [23]. Two quarter-scale RC columns equipped with longitudinal SMA reinforcement in their plastic hinge regions were subjected to shake table tests, and the results were compared to a similar RC column that had no SMA reinforcement. It was reported that the SMA-reinforced columns recovered almost all of their plastic deformation. In another study, Saiidi et al. [24] investigated the seismic performance of RC bridge columns reinforced with alternative materials, such as superelastic Ni-Ti SMA and engineered cementitious composites (ECCs). The experimental test results showed that the column specimens made with SMA longitudinal bars and ECC experienced the least damage and exhibited the highest drift capacity. A notable decrease in the residual drift was also recorded in the tested SMA-ECC specimens, with an average ratio of residual to maximum drift between 16% and 50% of that observed in the conventional RC column and the SMA-reinforced RC column.

Noguez and Saiidi [25] conducted shake table tests on a quarter-scale, three-span bridge model made with six columns to study the effect of advanced materials on reducing the permanent deformation and damage caused by earthquake loads. One pair of columns was fabricated with superelastic Ni-Ti SMA reinforcement in the bottom plastic hinge along with ECC, whereas the other two pairs of columns had post-tensioned steel rods, one with and the other without built-in

elastomeric rubber pads. The results of this experimental study showed that the bridge pier with SMA-ECC and the bridge pier with both post-tensioned steel rods and elastomeric rubber pads experienced minimal damage and permanent deformation. In contrast, the pier with only post-tensioned steel rods had less permanent deformations but suffered from severe concrete spalling and rebar rupture. Notably, bottom plastic hinges remained undamaged in the piers with SMA-ECC and elastomeric pads in their plastic hinges. Thus, the damage was mainly concentrated in the top plastic hinges as they were conventionally designed without using advanced materials.

Hosseini et al. [7] used superelastic Cu-SMA and ECC to strengthen RC bridge columns. The proposed design of the column comprised a prefabricated tube made with ECC and longitudinal and transverse rebars, where Cu-SMA rebars replaced the longitudinal steel rebars in the plastic hinge region of the column, as shown in Fig. 18. The results showed that the partial and complete replacement of steel rebars with Cu-SMA rebars reduced the permanent deformations of the column by up to 33% and 90%, respectively. However, the complete replacement of steel with SMA rebars resulted in a lower strength, stiffness, and energy absorption capacity than conventional RC columns. In contrast, the inclusion of ECC resulted in an increase in the lateral load capacity of the column by 15%. Tazarv and Saiidi [26] used superelastic Ni-Ti SMA rebars and ECC in the plastic hinge region of a half-scale precast bridge column specimen to improve its seismic performance compared to a cast-in-place column specimens made with conventional materials. The results showed that the precast column made with advanced materials experienced negligible damage compared to the cast-in-place column. Up to a drift ratio of 12%, only ECC cover spalling was observed in the precast SMA-equipped column, whereas concrete crushing and rebar buckling were evident in the cast-in-place column. The residual displacement of the precast column was reported to be 79% lower than that of the cast-in-place column, ensuring post-earthquake functionality of the column.

Varela and Saiidi [97] proposed a different concept for designing earthquake-resistant bridges, in which superelastic Ni-Ti SMA rebars were examined for self-centering and energy dissipation. The rebars were inserted in a replaceable plastic hinge fabricated of rubber, which was then attached to a concrete-filled CFRP tube. To evaluate the performance of the proposed concept, a quarter-scale model was subjected to near-fault earthquake ground motions on a shake table. A unique aspect of the proposed model is that it can be easily disassembled, reassembled, and retested after the first round of testing. The experimental test results showed that the specimen experienced a residual drift of 0.5% under a maximum drift ratio of 7%. Furthermore, the reassembled model exhibited the same force and drift capacity as the original model. In another study, Varela and Saiidi [46] evaluated the system-level performance of the bridge column concept proposed by Varela and Saiidi [97] by testing a quarter-scale, two-span bridge model using a shake table. The model consisted of three two-column bents, where the first bent was made with Cu-SMA rebars and ECC in the plastic hinge, while the second bent included Ni-Ti rebars and rubber plastic hinges. The last bent was made with a Ni-Ti rebar and ECC. They found that superelastic Ni-Ti and Cu-SMA rebars are effective in recentering bridge piers. In contrast, the inclusion of ECC and rubber minimized the damage, whereas the smallest residual deformations were observed in the bridge columns made with Cu-SMA rebars and ECC. The study also revealed that the original and reassembled models exhibited comparable force, drift, initial stiffness, and energy dissipation capacity.

The only study specifically focused on using superelastic SMA rebars for the strength enhancement of RC columns was that of Xing et al. [27]. In this study, the flexural performance of RC columns strengthened with NSM superelastic Ni-Ti SMA rebars with and without CFRP jackets was evaluated. Strengthening with the NSM SMA rebars increased the drift capacity of the columns, and this increase was further pronounced when the CFRP jacket was used in conjunction with the NSM SMA rebars. An increase in the energy dissipation and a decrease in the stiffness degradation were also reported upon strengthening with the NSM SMA rebars. The cited study concluded that the effectiveness of NSM SMA rebars can be improved by designing a system such that SMA rebars experience large strains. This helps them undergo a phase transformation, resulting in the activation of their superelastic behavior.

All studies conducted on the self-centering of RC columns have

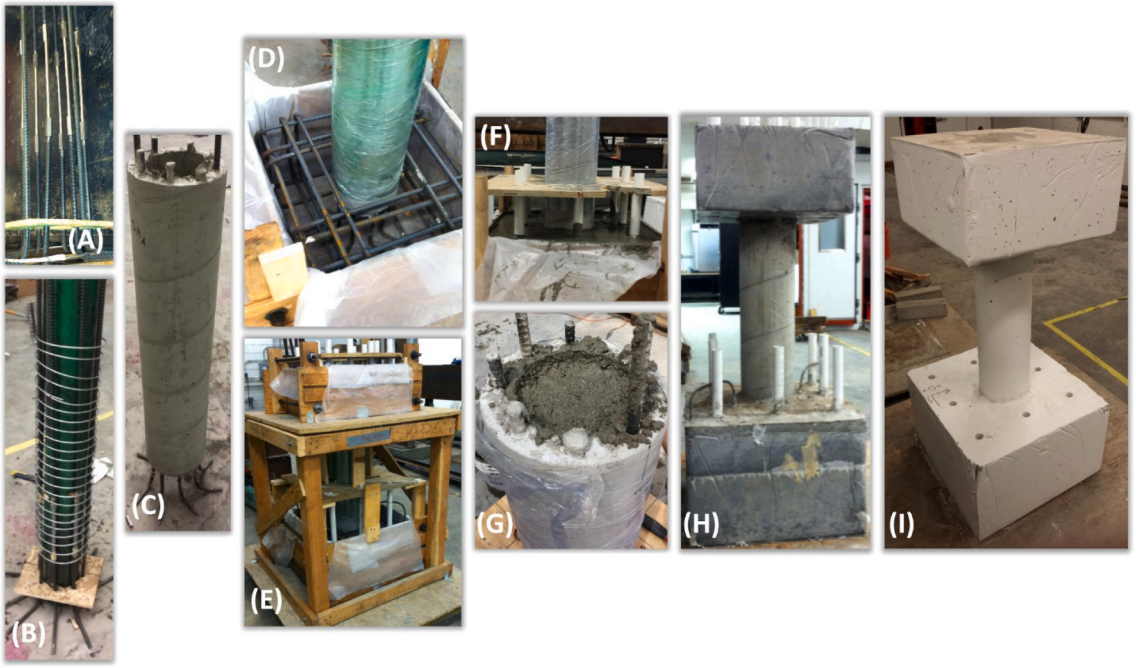

Fig. 18. Strengthening with superelastic Cu-SMA rebars: (a) coupling of Cu-Al-Mn SMA rebars with steel rebars using mechanical couplers, (b) placing the transverse spiral reinforcement inside the formwork, (c) pre-fabricated reinforced ECC tube, (d) placing the reinforced ECC tube inside the foundation's rebar cage, (e) assembling the formwork, (f),(g) placing conventional concrete inside the foundation and prefabricated tube, (h) specimen after removal of the formwork, and (i) specimen ready for testing after surface finishing [7-IOP Publishing Ltd Copyright].

utilized superelastic SMA rebars as internal column reinforcements. A detailed review of these studies shows that complete replacement of steel with SMA rebars can reduce the residual displacements by more than 90%, and thus, can be effective in recentering RC columns under strong lateral motions. However, a drawback associated with this approach is that such columns exhibit a strength, stiffness, and energy dissipation that are lower than those of their conventional counterparts. The partial replacement of steel with superelastic SMA rebars is a possible alternative to overcome this issue. Similarly, advanced materials, such as ECC and ultra-high-performance concrete, can be used in conjunction with superelastic SMA rebars to achieve an energy dissipation capacity comparable to that of conventional columns. Furthermore, it should be highlighted that the configurations developed in the existing studies are most suitable for the design of new columns. The utilization of the SME of SMA rebars, particularly Fe-SMA rebars, to prestress existing RC columns is a promising strengthening solution that has not been explored to date. The SMAs that exhibit a notable SME can be used in the form of either bonded or unbonded reinforcement for prestressing the columns to reduce their residual deformations. Future studies are recommended to investigate the potential of this strengthening approach further.

4.2.2. *Confinement using shape memory effect*

SMAs can be provided in the form of embedded or external spirals and wire jackets to improve the confinement of RC columns. Specifically, the recovery stress generated by the SME of SMAs can be utilized for active confinement of RC columns. This leads to improved ductility and energy dissipation capacity, as opposed to the passive confinement provided by conventional steel spirals. A comparative study on the lateral behavior of RC columns retrofitted with Ni-Ti-Nb SMA spirals and those with GFRP wraps was conducted by Shin and Andrawes [41]. The retrofitting scenarios considered are shown in Fig. 19. The experimental test results showed a significant increase in the displacement ductility (up to three times), energy dissipation (up to four times), and equivalent viscous damping ratio (up to 1.5 ×) of the SMA-retrofitted columns compared to the GFRP-retrofitted columns. Furthermore, the SMA-retrofitted columns experienced far less damage than the reference and GFRP-retrofitted columns. The cited study concluded that SMA spirals are effective in improving the seismic performance of vulnerable RC columns and can be used to ensure functionality of bridges after a major earthquake event. In another study, Shin and Andrawes [17] evaluated the feasibility of repairing RC columns using Ni-Ti-Nb SMA spiral wires. To this end, two 1/3-scale severely damaged RC columns were considered. The 6% prestrained SMA spirals were wrapped around the plastic hinge region of the specimens and then activated by heating to 100 °C. The test results showed that the repair using SMA spirals restored the lateral strength and enhanced column ductility. Furthermore, the initial stiffness of the repaired columns increased by 150%. The cited study noted that the amount of SMA required to significantly improve the behavior of the columns remains small.

Choi et al. [16] used Ni-Ti SMA and Ni-Ti-Nb SMA wires to retrofit RC columns with lap splices. The study first investigated the recovery and residual stresses, which were found to be 354 MPa and 216 MPa, respectively, for Ni-Ti-Nb wires at 6% prestrain, and 223 MPa and 27 MPa, respectively, for Ni-Ti wires at 5% prestrain. Subsequently, SMA wires were employed to retrofit RC columns. The prestrained SMA wires were wrapped and fixed in the plastic hinge of the columns using two anchors and then activated by heating to 200 °C. The drift capacity of the strengthened columns was found to be up to three times greater than that of the unstrengthened columns. The efficacy of Ni-Ti SMA and Ni-Ti-Nb SMA wires in improving the ductility of the columns was similar overall. However, the cited report recommended using Ni-Ti-Nb SMAs for civil engineering structures, as they offer a more suitable temperature range for activation. Recently, Jung et al. [42] evaluated the seismic performance of RC columns retrofitted with Ni-Ti-Nb SMA spirals, as shown in Fig. 20. The SMA spirals were prestrained up to 6.5% and then thermally activated, resulting in a recovery stress of 447 MPa. Under bidirectional lateral loads, retrofitted columns exhibited greater ductility and smaller residual deformations than the unretrofitted column while sustaining a drift ratio of 10.5% without concrete crushing. The unretrofitted column was subsequently repaired with SMA spirals after experiencing damage. The applied repair helped the damaged column regain its seismic capacity while preventing further damage under lateral loads.

A review of the relevant studies shows that the active confinement provided by the SME of SMAs can be effective in enhancing the drift

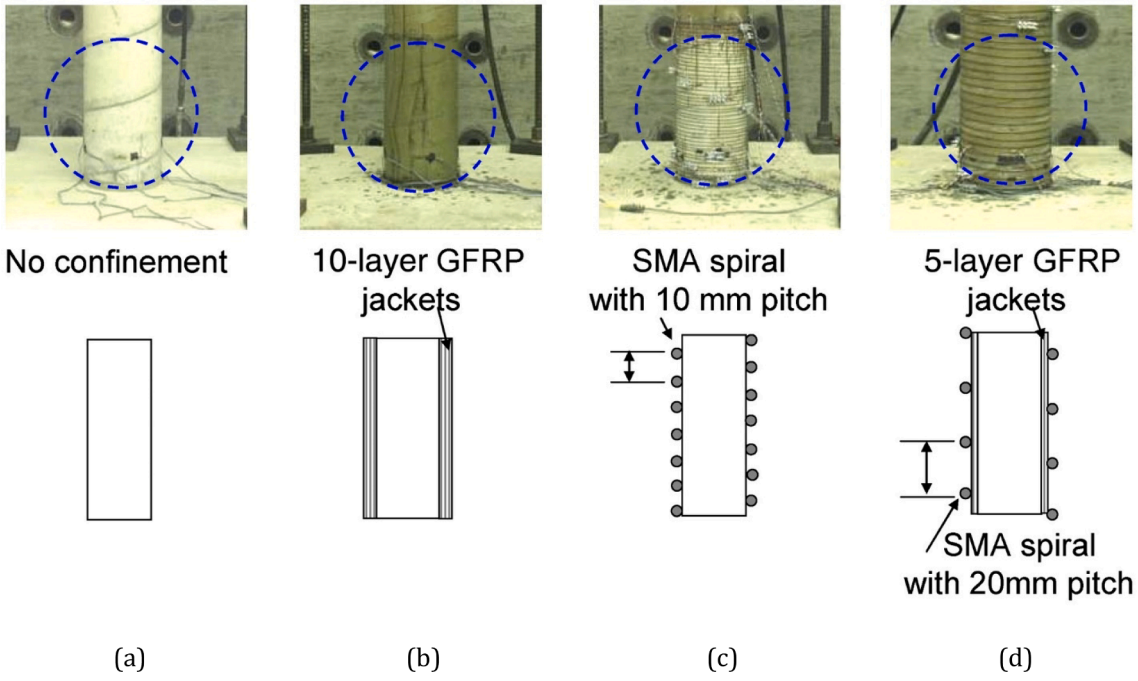

Fig. 19. As-built and retrofitted columns with SMA and GFRP [41-With permission from ASCE].

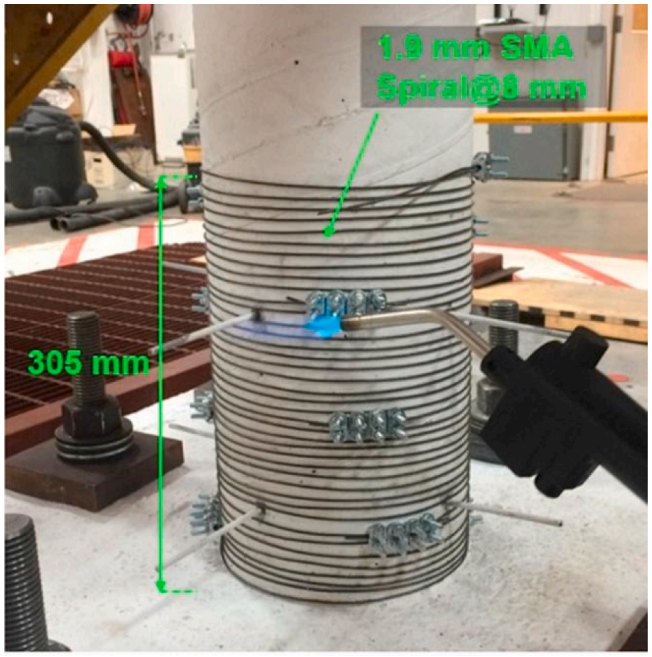

Fig. 20. Retrofit of a RC column with Ni-Ti-Nb SMA spirals [42-Elsevier copyrights].

capacity and energy dissipation of deficient RC columns. The active confinement pressures used in previous studies ranged from 0.4 to 2.0 MPa. In particular, an active confinement pressure of 1.2 MPa is sufficient to increase the energy dissipation capacity of a column by up to four times [17]. Another important aspect is the reduction of residual deformations in the columns owing to the active confinement provided by SMA spirals. This is because the transfer of damage to the reinforcing rebar is delayed owing to the active confinement of the concrete core. Noting that all existing studies have employed Ni-Ti-Nb SMA spirals for active confinement of RC columns, the potential of Fe-SMA for the active confinement of RC columns is an interesting research topic that should be investigated in future studies.

4.3. Beam-Column joints

Joints are considered the most critical regions in RC structures, where any deficiency can lead to catastrophic failure. The common deficiencies in RC beam-column joints include poor-quality concrete and lack of shear reinforcement, especially in structures designed and constructed before the development and implementation of modern seismic design codes. Such joints are expected to experience severe permanent damage under earthquake-induced forces, which may ultimately lead to collapse of the entire structure. The superelastic properties of SMAs can be exploited to reduce residual deformations in the plastic hinge region of beam-column joints. Most existing studies on the use of SMA in beam-column joints have proposed replacing the steel rebars in the plastic hinge region of the beam-column joint with SMA rebars. A summary of the existing studies on the application of SMAs in RC beam-column joints is presented in Table 5. The studies are categorized based on the purpose of strengthening, that is, self-centering and/or shear strengthening.

4.3.1. Self-Centering using superelasticity

Most relevant studies on beam-column joints have utilized superelastic SMAs to add self-centering behavior to the joint under earthquake loads. For this purpose, the SMA is commonly provided as an internal reinforcement in the plastic hinge region of beam-column joints. In previous studies, Youssef et al. [28] investigated the seismic behavior of an RC beam-column joint reinforced with superelastic Ni-Ti SMA rebars in the plastic hinge region. The details of the SMA-reinforced specimens are shown in Fig. 21. The SMA-reinforced joint exhibited a residual drift ratio of 1.98%, compared to 4.94% recorded in a conventional joint of similar dimensions. While the use of SMA rebars moved the plastic hinge region away from the face of the column, the energy dissipated by the SMA-reinforced specimen was reported to be less than that dissipated by the conventional joint.

Nehdi et al. [29] proposed a hybrid SMA-FRP beam–column joint to improve the seismic performance of a joint panel while ensuring adequate corrosion resistance. Two joint panels were considered, and steel rebars were provided in one of them. In the other panel, SMA rebars were provided in the plastic hinge region, and GFRP rebars were included in the rest of the joint. A similar force–displacement hysteretic response was reported for the two specimens, wherein the specimen with the SMA rebars exhibited less stiffness but similar residual drift, compared to the steel-reinforced specimen. The comparable residual drift was attributed to the significant slippage of the GFRP rebars inside the couplers. However, notably, the SMA-reinforced specimen could carry 89% of its maximum load capacity even after the collapse limit (i.e., 3% story drift). The use of SMA rebars relocated the plastic hinge region away from the face of the column. In another study, Nehdi et al. [30] subjected an RC beam-column joint reinforced with Ni-Ti SMA rebars in the plastic hinge region to cyclic lateral loads. The damaged specimen was subsequently repaired with flowable shrinkage-compensating repair concrete and then retested. The experimental test results showed that SMA-reinforced beam-column joints can recover

Table 5
Summary of the studies on RC beam-column joints equipped with SMAs (sorted in a chronological order).

Study - Year	Technique	Property Used	Type of Loading	Comparison with Control Specimen		
				Strength	Energy Dissipation	Residual Displacement
Youssef et al. [28] – 2008	Ni-Ti SMA internal reinforcement in the plastic hinge region	SE	Quasi-static reversed cyclic loading	=	↓	↓
Nehdi et al. [29] – 2010	Ni-Ti SMA internal reinforcement in the plastic hinge region and FRP bars in the other regions	SE	Quasi-static reversed cyclic loading	=	=	=
Nehdi et al. [30] – 2011	Ni-Ti SMA internal reinforcement in the plastic hinge region and repair with shrinkage-compensating concrete	SE	Quasi-static reversed cyclic loading	NR	NR	↓
Oudah and El-Hacha [31] – 2017	Ni-Ti SMA internal reinforcement anchored using screwlock steel anchors	SE	Quasi-static cyclic loading	↓	NR	NR
Oudah and El-Hacha [32] – 2018	Ni-Ti SMA internal reinforcement in the plastic hinge region	SE	Quasi-static reversed cyclic loading	=	↓	↓
Yurdakul et al. [33] – 2018	Externally applied diagonal post-tensioned Ni-Ti SMA rods	SE	Quasi-static reversed cyclic loading	↑	↑	NR
Oudah and El-Hacha [98] – 2020	Ni-Ti SMA internal reinforcement in the plastic hinge region	SE	Quasi-static reversed cyclic loading	NR	NR	↓

Notations: SE, superelasticity; SME, shape memory effect; NR, not reported; ↑, increased; ↓, decreased; =, same

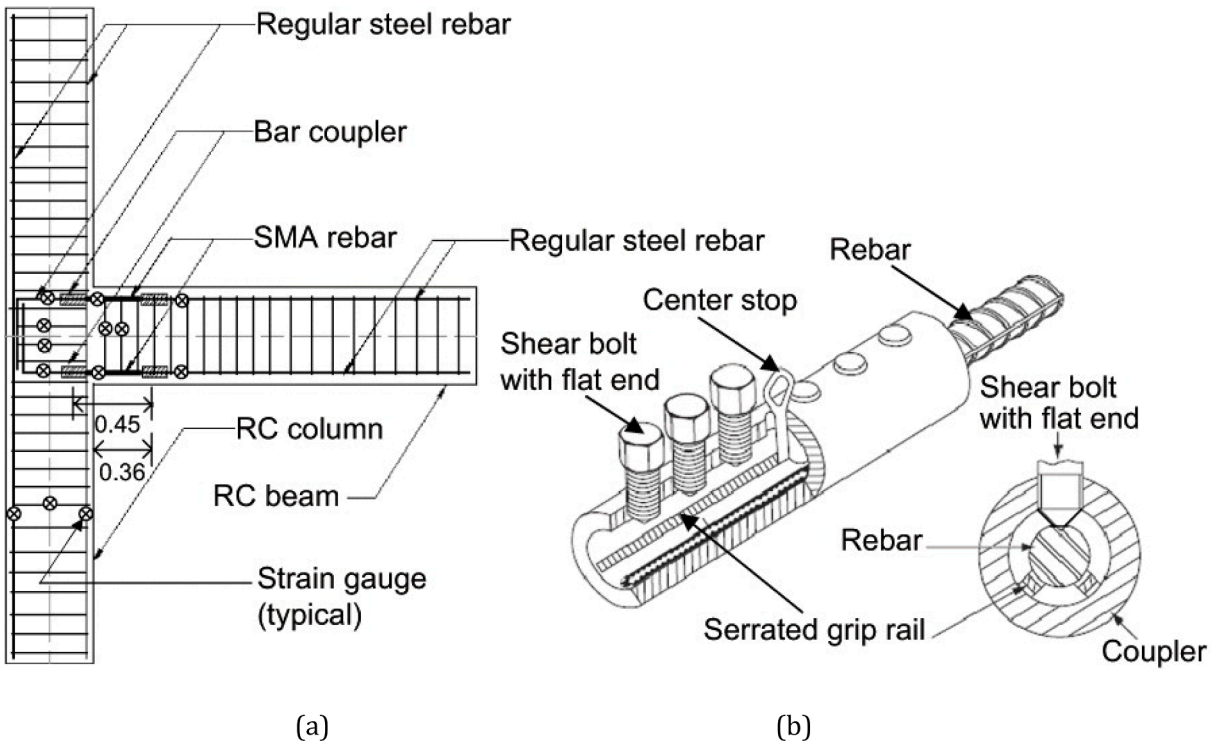

Fig. 21. Reinforcing details used for the beam-column joint with superelastic Ni-Ti SMA rebars: (a) detailing with SMA and regular steel rebars, and (b) single-barrel screw-lock coupler used for connecting the SMA rebar to the steel rebar [28-Copyrights Taylor and Francis].

nearly all of the permanent deformations that they experience under earthquake loads, and thus require only minimal repair. Furthermore, the energy dissipation capacities of the repaired and original specimens were comparable, and the plastic hinges of the specimens were developed away from the face of the column.

Oudah and El-Hacha [31] evaluated the performance of RC beam-column connections reinforced with superelastic Ni-Ti SMA rebars. The rebars were anchored to the joints using screw-lock steel anchors. Six beam-column joint specimens were considered, where four of the specimens were reinforced with SMA rebars and the remaining two were reinforced with steel rebars. The experimental test results revealed that SMA-reinforced connections exhibited a significantly lower ultimate force capacity than steel-reinforced specimens, which was due to the slippage and fracture of the SMA rebars. It was also reported that increasing the anchorage depth in the joint enhanced the post-cracking stiffness and reduced the ultimate curvature of the specimens. In another paper, Oudah and El-Hacha [32] proposed a solution for retrofitting beam-column connections by moving the plastic hinge region away from the face of the column. For this purpose, a vertical slot was inserted at a distance equal to the effective depth from the end of the beam, and the connection was reinforced by superelastic Ni-Ti SMA rebars, as shown in Fig. 22. Three specimens were considered: one was a control specimen with conventional detailing and the other two were detailed with SMA and steel rebars, along with a vertical slot in the beam. The SMA-reinforced beam-column connection demonstrated superior performance in terms of self-centering, reducing the joint distortion, minimizing the pinching shear effect, and relocating the plastic hinge region, compared to the control specimen. Furthermore, the specimen made

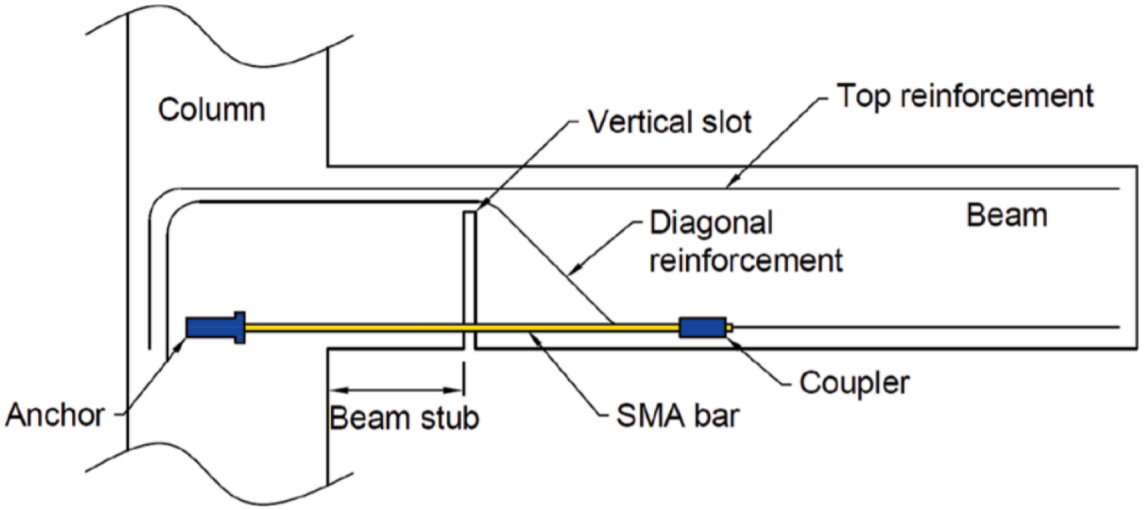

Fig. 22. Schematics of the strengthening technique used for the beam-column joint with SMA rebars [32-Authorized Reprint from American Concrete Institute].

with SMA rebars recovered most of the residual displacements and exhibited a drift capacity higher than that of the other two specimens tested.

More recently, Oudah and El-Hacha [98] proposed an SMA-reinforced double slotted beam-column connection to relocate the plastic hinge away from the face of the column and compared it with the single slotted connection proposed in [32]. The double (top and bottom) vertical slots were placed away from the face of the column at a distance equal to the effective depth of the beam. The SMA rebars were then placed in the plastic-hinge region. The advantages of this technique include the relocation of the plastic hinge and the mitigation of damage to the slab attached to the beam by including an expansion joint at the location of the vertical slots. The experimental test results showed a self-centering response of the connection at drifts of up to 14%.

4.3.2. Shear strengthening using superelasticity

Yurdakul et al. [33] explored the retrofitting of shear-deficient beam-column joints using externally applied, post-tensioned superelastic Ni-Ti SMA rebars placed diagonally, as shown in Fig. 23. To this end, three deficient beam-column joint subassemblies were developed, wherein the first specimen served as the reference specimen and the other two were retrofitted with post-tensioned SMA and steel rebars. The specimens were subjected to cyclic loads with a drift ratio of up to 8%. The reference specimen experienced brittle shear failure, whereas the specimen retrofitted with SMA rebars exhibited ductile behavior with minimal damage to the joint panel. In addition, the ultimate lateral load-carrying capacity of the specimen retrofitted with SMA rebars was significantly higher than that of the other two specimens. The cited study concluded that SMA rebars should be post-tensioned up to their yield capacity to further improve the performance of this retrofitting scheme.

A holistic overview of the experimental studies conducted on the SMA-reinforced beam-column joints indicated that the use of superelastic SMA rebars in the beam-column joint region can reduce the residual displacements by more than 60%. However, such beam-column joints dissipate less energy. To overcome this issue, superelastic SMAs should be used along with advanced materials in the plastic hinge region of the joint. Shear strengthening of deficient beam-column joints can also be achieved using post-tensioned superelastic rebars, which improves the ductility and load capacity of the joints. Notably, no study has so far utilized the SME of SMA rebars and spirals for prestressing beam-column joints to improve their self-centering and ductility. Future studies should address this research gap.

4.4. Shear walls

Shear walls serve as the primary lateral load resisting system in a wide range of low- to high-rise buildings. The imposed lateral loading demand is dissipated in the plastic hinge region of the shear walls, resulting in permanent damage in these regions. Superelastic SMAs can effectively reduce the residual displacements of RC shear walls during an earthquake, and thus, can help achieve self-centering. Furthermore, flexural and shear strengthening of RC walls can be accomplished by exploiting the SME of SMAs. The number of studies that have utilized SMAs to strengthen RC shear walls is limited. Details of the available studies are listed in Table 6. The studies were categorized based on the technique employed (i.e., SMA braces and SMA longitudinal rebars) to incorporate the self-centering behavior into RC shear walls.

Fig. 23. Shear strengthening using post-tensioned superelastic Ni-Ti SMA rebars [33-Springer copyrights].

4.4.1. Self-Centering using superelasticity of SMA braces

Effendy et al. [91] proposed a bracing system comprising SMA rebars to increase the energy dissipation and ductility of low-rise RC shear walls. Three wall specimens were considered for this purpose, including a control specimen, a superelastic SMA-reinforced specimen, and a martensitic SMA-reinforced specimen activated at 150 °C. The SMA rebars were placed as external bracings on both sides of the walls. The experimental study showed that the martensitic SMA-reinforced specimen had a greater residual displacement compared to the specimen with superelastic SMA rebars. Furthermore, one of the four superelastic SMA rebars buckled at the ultimate load, which resulted in less energy dissipation than expected. The cited study concluded that the prevention of buckling of SMA rebars, when provided as external bracings, can be a potential challenge that needs further investigation.

In another study, Cortés-Puentes and Palermo [36] explored the retrofitting of deficient squat RC walls using superelastic Ni-Ti SMA braces, as shown in Fig. 24. Short diagonal SMA links connected to rigid steel elements were provided as resettable fuses in the retrofitted walls. This retrofitting technique was reported to significantly reduce damage at the base of the wall. In addition, the lateral strength of the retrofitted wall was enhanced (compared to the control wall) owing to the tension force developed in the braces. The drift capacity of the retrofitted specimen, controlled by diagonal tension cracks, also improved. However, the retrofitted specimen controlled by shear sliding did not experience an increase in drift capacity, mainly because the behavior of both the reference and retrofitted walls was controlled by base rocking. The cited study concluded that additional retrofitting may be needed in walls that undergo shear sliding, especially to reduce localized cracks and base rotations.

4.4.2. Self-Centering using superelasticity of SMA longitudinal rebars

Abdulridha and Palermo [34] evaluated the performance of superelastic Ni-Ti SMA rebars in improving the seismic behavior of RC shear walls. To this end, two ductile RC shear walls were tested under quasi-static lateral loads. The first setup was designed as an RC specimen with steel rebars, whereas the steel rebars in the plastic hinge region of the other specimen were replaced with SMA rebars, as shown in Fig. 25. A displacement recovery capacity of 92% was reported for a shear wall that contained SMA rebars, in contrast to a displacement recovery capacity of 31% recorded in a conventional RC wall. In contrast, the lateral strength and displacement capacity of the shear wall with SMA rebars were similar to those of a conventional RC wall. However, the energy dissipated by the RC wall specimen was higher, mainly because of the flag-shaped hysteresis of the superelastic SMA rebars, which resulted in less energy dissipation in the shear wall made with SMA rebars.

Cortés-Puentes et al. [35] repaired the damaged slender concrete walls used in Abdulridha and Palermo [34] and then tested them under quasi-static cyclic loads. The repair process included the removal of damaged concrete, replacement of buckled steel rebars, shortening of SMA bars, and placement of high-strength self-consolidating concrete. The experimental test results showed that the wall repaired with SMA rebars exhibited self-centering and recovered up to 80% of its residual displacements until a drift ratio of 2% was achieved. The pinching effect in the wall repaired with SMA rebars was also greater than that in the

Table 6
Summary of the studies on RC shear walls equipped with SMAs (sorted in a chronological order).

Study - Year	Technique	Property Used	Type of Loading	Comparison with Control Specimens			
				Strength	Stiffness	Ductility	Residual Displacement
Effendy et al. [91] – 2006	SMA rebars as external braces	SE and SME	Quasi-static reversed cyclic loading	↑	NR	↑	↓
Abdulridha and Palermo [34] – 2017	Ni-Ti SMA rebars as internal longitudinal reinforcement in the plastic hinge region	SE	Quasi-static reversed cyclic loading	↓	↓	=	↓
Cortés-Puentes et al. [35] – 2018	Ni-Ti SMA internal reinforcement in the plastic hinge region	SE	Quasi-static reversed cyclic loading	=	=	NR	↓
Cortés-Puentes and Palermo [36] – 2018	Ni-Ti SMA rebars as external braces	SE	Quasi-static reversed cyclic loading	↑	↑	↑	↓
Yan et al. [59] – 2018	Fe-SMA rebars as internal longitudinal reinforcement	SE	Quasi-static reversed cyclic loading	↓	↓	NR	NR
Kian and Noguez [37] – 2018	Ni-Ti SMA internal reinforcement in the boundary element	SE	Quasi-static reversed cyclic loading	=	↓	↑	↓
Almeida et al. [38] – 2020	Ni-Ti SMA internal reinforcement in the boundary element	SE	Quasi-static reversed cyclic loading	↓	NR	↑	↓

Notations: SE, superelasticity; SME, shape memory effect; NR, not reported; ↑, increased; ↓, decreased; =, same

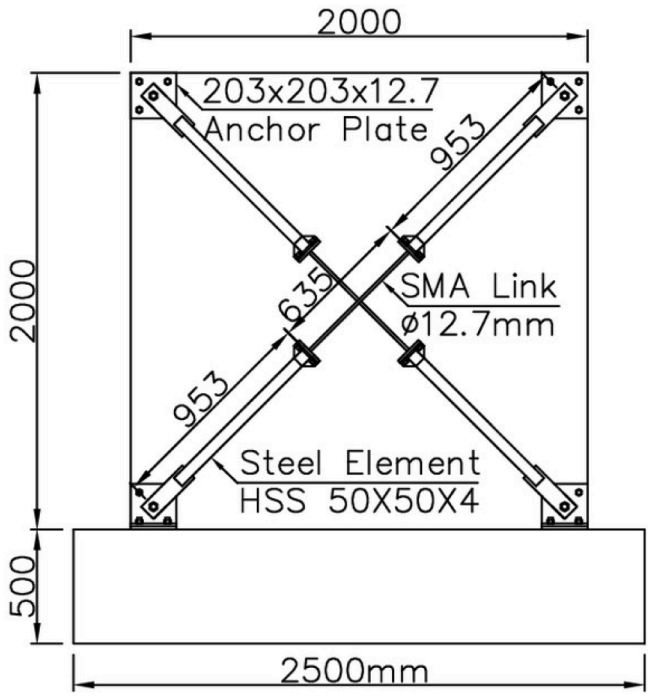

Fig. 24. Retrofitting of a RC shear wall with superelastic Ni-Ti SMA braces [36- With permission from ASCE].

wall repaired with steel. The hysteretic response of the wall repaired with SMA rebars was symmetric because of the recentering effect, as opposed to the unsymmetrical response of the wall with no SMA rebars. Similarly, Yan et al. [59] compared the seismic performance of conventional shear walls with superelastic Fe-SMA-reinforced shear walls. This study investigated the effect of the steel stirrup ratio and SMA reinforcement ratio on the performance of the walls. An increase in the cracking, yield, and ultimate load capacity of the SMA-reinforced walls was observed. In addition, the seismic resistance, defined in terms of the ratio of the residual force to the maximum force in each cycle, of the SMA-reinforced walls was found to increase by more than 20% compared to that of the conventional shear walls. For a given reinforcement ratio, the shear walls reinforced with small-diameter SMA rebars performed better than the shear walls reinforced with large-diameter SMA rebars.

Three schemes were evaluated by Kian and Noguez [37] to mitigate the damage to RC shear walls during an earthquake. Four specimens were considered, including a control conventional RC wall specimen, GFRP-ECC, post-tensioned steel fiber reinforced concrete (SFRC), and SMA-SFRC wall specimens. The experimental study showed that the hybrid combination of steel bars and self-centering reinforcement reduced the permanent deformations of the specimens compared to the control specimen, while maintaining a similar ductility and energy dissipation. It was also reported that the GFRP- and SMA-reinforced shear walls exhibited improved self-centering behavior after a drift ratio of 1.0%, whereas the specimen with the post-tensioned tendons showed self-centering from the beginning of the test. The cited study noted that the SMA-SFRC shear wall exhibited the highest drift capacity among all the specimens tested. More recently, Almeida et al. [38] studied the self-centering and damage mitigation of flexure-controlled RC walls reinforced with superelastic Ni-Ti SMA rebars in the plastic hinge region. The experimental study showed that the specimen with SMA rebars failed at a drift ratio above 2.0%, while the specimen without SMA rebars failed at a drift ratio not exceeding 1.4%. The residual displacements of the specimen with SMA rebars were also (on average) one-third of the RC specimen. In addition, a displacement recovery capacity of 75% was observed for the specimen with SMA rebars; therefore, the residual drifts were maintained below the standard limit of 0.5% [114].

A synthesis of the available studies shows that the superelastic SMA, when provided as an internal reinforcement, can help recover up to 90% of the residual displacements in RC shear walls. However, this results in a reduction in the energy dissipation capacity of the RC shear walls. In contrast, superelastic SMA used as an external reinforcement increases the energy dissipation and drift capacity, while it reduces the residual displacements by up to 50%. The SME of SMAs has not yet been exploited to prestress RC walls for self-centering. It is expected that the prestressing of RC walls using the SME of bonded SMAs can help achieve self-centering, along with a reasonable energy dissipation capacity.

5. Design guidelines for SMA reinforced structures

The development of design codes and guidelines is essential for facilitating the expansion of SMA use in practice. Despite the variety of experimental studies that have demonstrated the effectiveness of SMA, there is only a limited amount of work on the development of design guidelines for SMA-reinforced structures. Saiidi et al. [99–100] proposed design guidelines for superelastic Ni-Ti SMA-reinforced ECC bridge columns and superelastic Ni-Ti SMA-reinforced FRP-confined concrete bridge columns. With reduced residual displacements, such columns were recommended for regions with seismic design categories of “C” and “D,” according to AASHTO [101]. The design methodology was recommended to be displacement-based, instead of the force-based

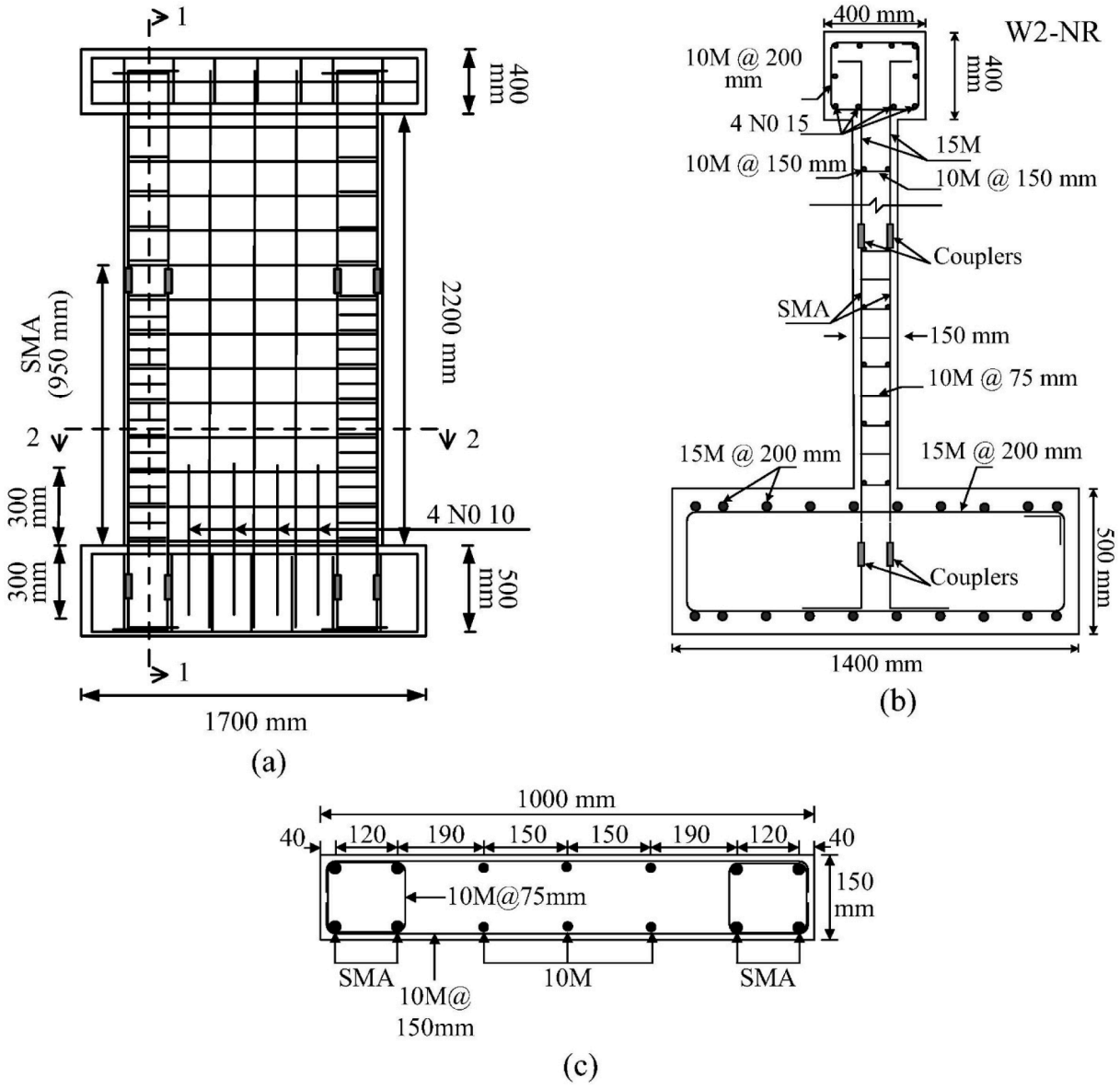

Fig. 25. Reinforcement details of the wall made with superelastic SMA rebars: (a) elevation view, (b) section 1–1, and (c) section 2–2 [34-Elsevier Copyrights].

method used for conventional RC columns. The damping ratio was proposed to be 3.2%, instead of 5.0%. This was because of the low hysteretic damping observed in columns with low residual displacements. In contrast, the displacement demand was proposed to increase by 20% compared to conventional columns to account for low damping. The minimum and maximum amounts of SMA reinforcement for such columns were recommended to be 1% and 4%, respectively. The maximum recommended design axial load ratio was 0.15. The minimum drift capacity proposed for flexure-dominated (i.e., wall aspect ratio = 4) SMA-reinforced ECC columns was 2.0%. Similarly, the recommended minimum lateral strength was equal to 10% of the axial load expected for the columns.

A performance-based seismic design methodology was also proposed for superelastic Ni-Ti SMA-reinforced RC bridge piers by Billah and Alam [102–103]. According to the proposed methodology, the serviceability requirement is met when the residual drift is below 0.25%. In contrast, a residual drift greater than 1% resulted in the damage state of collapse for the superelastic SMA-reinforced RC bridge piers. Note that most of the existing work on the development of design guidelines for SMA-reinforced RC structures focusses on the design of new RC bridge piers reinforced with superelastic SMAs, and guidelines for the strengthening of existing structures with SMAs are almost non-existent. Thus, it is critical to develop guidelines to facilitate the use of SMAs in the field for various strengthening applications.

6. Comparison and discussion

The extensive literature review systematically discussed in the previous sections shows that the use of SMA as a longitudinal reinforcement embedded in RC structures can help recover the plastic deformations, thereby leading to self-centering behavior, which contributes to ensuring the immediate functionality of the structure after extreme loading events. In addition, external strengthening with longitudinal SMA rebars resulted in enhanced flexural strength and stiffness of the structure. In contrast, the utilization of SMA as a transverse reinforcement in the form of wire jackets or spirals can lead to the effective confinement of RC structural components, resulting in the enhancement of their ductility and energy dissipation capacity. This section first presents an overview of the availability of SMA products in different formats and then compares the effectiveness of different types of SMA

for strengthening RC structures. Furthermore, a side-by-side comparison of SMA strengthening with other conventional strengthening techniques is provided.

6.1. Product formats available for different SMAs

From past studies and real-world applications, SMA products were found to be used in different formats. Superelastic Ni-Ti SMAs have been frequently used as wires, plain rebars, threaded rebars, and cables, whereas Ni-Ti-Nb and Cu-Al-Mn SMAs have so far been used only in the form of wires and plain/threaded rebars, respectively. In contrast, Fe-SMA is available in a variety of formats (i.e., wire, plain rebar, threaded rebar, ribbed rebar, and strip, excluding cable). Table 7 provides the range of dimensions available for the different formats of SMA products.

6.2. Strengthening using different SMAs – Pros and cons

The highest elastic modulus among the four SMA types widely investigated to date has been delivered by Fe-SMAs. Thus, Fe-SMAs have the highest tendency to resist deformation compared to the other SMAs. Furthermore, Fe-SMAs have a low cost, good machinability, and simple manufacturing process. In contrast, nickel-based SMAs are expensive and suffer from poor machinability, while copper-based SMAs have excellent machinability and are cost-effective but offer a low elastic modulus. Considering all these factors, Fe-SMAs can be considered a promising choice for the strengthening and repair of existing structures, as well as for prestressing new structures. However, notably, a disadvantage associated with Fe-based SMAs is their relatively low recovery strain, especially compared to nickel- and copper-based SMAs.

The results from the previous studies available in the literature show that Ni-Ti and Cu-SMA are more suitable for use as internal, external, or embedded reinforcements in RC structural components to achieve self-centering behavior, owing to their superelasticity. Superelastic SMAs, when included as an internal reinforcement, can recover up to 90% of the residual deformation of the structure. However, notably, the inclusion of SMAs as an internal reinforcement can reduce the energy dissipation capacity and stiffness of the structure by up to 50% owing to their flag-shaped hysteresis response and low elastic modulus. Therefore, advanced materials, such as ECC and ultra-high-performance concrete, need to be used in conjunction with superelastic SMAs to achieve adequate energy dissipation, along with self-centering. Conversely, a combination of steel and SMA rebars can be used for reasonable energy dissipation and stiffness, along with the ability to partially recover deformations.

Ni-Ti-Nb SMA and Fe-SMA are more suitable for use as external or embedded reinforcements for prestressing and confining RC structures because of excellent SME exhibited by them. The recovery stress generated by the SME can significantly improve the serviceability of RC structures, especially by reducing the cracks and deflections that could potentially impair the functionality of the structure. The increase in the cracking load resistance has been reported to be up to 265%, depending on the strengthening technique. Prestressing with Ni-Ti-Nb and Fe-SMAs can also help achieve self-centering behavior by increasing the axial load on the structure. Furthermore, as these SMAs do not exhibit a flag-shaped hysteresis response, they can result in adequate energy dissipation, as opposed to superelastic SMAs, in which there is a trade-off between self-centering and energy dissipation.

The active confining pressure resulting from the SME of Ni-Ti-Nb and Fe-SMAs makes them appropriate for the shear strengthening and confinement of RC structural components. According to past studies, the use of these SMAs in the form of spirals or braces can increase the shear capacity by up to 86%. The energy dissipation and drift capacity can also be significantly improved by the active confinement of these SMAs. In contrast, superelastic SMAs are not deemed effective primarily because they exhibit a passive confining pressure. Notably, Fe-SMAs are more suitable than Ni-Ti-Nb SMAs for strengthening applications involving SMEs, mainly because of their higher elastic modulus. Regarding the constructability aspects and field applications, superelastic SMAs (Ni-Ti and Cu-SMA) are relatively easy to install in the field as they do not need to be thermally activated. However, the on-site thermal activation of Ni-Ti-Nb and Fe-SMA requires specialized expertise and equipment. In previous studies, the latter SMAs were thermally activated using various methods, including electrical resistivity, infrared, fire torch, propane torch, and heating jacket. The heating of SMAs can be monitored using thermocouples and temperature sensors.

6.3. Strengthening using SMAs vs other techniques – Pros and cons

Strengthening with SMAs offers several advantages over existing strengthening techniques. Most importantly, SMAs have an easy installation process. Mechanical jacks, anchor heads, ducts, and hydraulic devices that are required for prestressing using CFRP or steel tendons are not required when prestressing with SMAs as they can be activated by heating. In addition, in contrast to other prestressing techniques, no frictional losses occur in the prestressing provided by SMAs owing to the development of a uniform tension force along their total length. This implies that SMAs can be conveniently used for prestressing not only straight but also curved concrete members [51]. Conventional FRP prestressing techniques involve strength-ductility trade-off due to the brittle nature of FRP, whereas owing to the ductile nature of SMAs, the ductility of the strengthened structural component is improved, in addition to the strength enhancements [53].

In terms of material usage, a small amount of SMA (i.e., reinforcement ratio $\leq$ 1.0%) can significantly improve the flexural and shear behaviors of RC structures. Furthermore, minimal labor is required for installing SMAs as opposed to other prestressed retrofitting techniques [30,42]. In contrast, traditional techniques, such as those involving concrete, steel, and FRP jackets, are often labor-intensive and time-consuming, which can delay the opening of the damaged structure after extreme events. For example, the time required for curing the resin used for the repair with FRP sheets can be up to a week, which is significant, compared to strengthening using SMA wires/spirals, which can be completed in<24 h [17]. In addition, SMA jackets do not require grouting, in contrast to the steel jackets used in RC structures. Other benefits associated with SMA strengthening include corrosion-resistant behavior, especially for Ni-Ti SMA, which offers a corrosion performance similar to that of stainless steel [12]. Furthermore, there is no danger of SMA reinforcement peeling off, as SMA jackets are anchored to

Table 7
Details of commonly available/used SMA products.

SMA Type	Wire Diameter (mm)	Plain and Threaded Rebars Diameter(mm)	Ribbed Rebar Diameter(mm)	Strip Width/Thickness (mm)	Cable Diameter (mm)
Ni-Ti SMA [16,18–19,21,24,27–28,92–95]	1.0, 2.0, 2.5, 3.0, 3.5	9.5, 12.0, 12.7, 15.9, 20.0, 32.0	NR	NR	1.6, 2.5, 5.6, 8.0
Ni-Ti-Nb SMA [16,40–42]	1.0, 2.0, 1.9, 3.9	NR	NR	NR	NR
Fe-SMA [50,51,54,56,79,81]	0.5, 1.0, 3.0	14.3, 18.0	8.0, 10.0, 12.0, 16.0	20/1.7, 120/1.5, 50/0.5, 50/1.5, 50/2.3	NR
Cu-Al-Mn SMA[43–44,46]	NR	4.0, 6.0, 10.0, 12.0	NR	NR	NR

Notations: NR = Not Reported.

the structure, contrary to the FRP jackets that are often bonded using adhesives. A main advantage of SMAs over other strengthening materials is that, owing to their high recovery stain and superelastic nature, they help reduce residual deformations in RC structures. This property is particularly useful for designing RC structures to resist extreme loads. Despite all the positive contributions, the drawback of using SMAs for strengthening purposes is their low elastic modulus, particularly for Ni- and Cu-based SMAs. Fe-based SMAs, in contrast, have a higher initial elastic modulus, although the elastic modulus is reduced upon loading after activation [64]. This is an important aspect that needs to be considered when exploiting the SME of Fe-based SMAs.

A recent field application of SMAs involved the strengthening of the negative moment area of a concrete slab in the basement of a Kasinopark in Aarau Switzerland [105–106]. As part of the renovation project, new column supports had to be built on the concrete slab, which had insufficient tensile and punching shear reinforcement. Prestressed Fe-SMA strips were used to address this deficiency and strengthen the concrete slab. Grooves were first cast onto the concrete surface, followed by fixing the Fe-SMA strips to the concrete surface using end anchorages. The strips were then activated using a custom-designed infrared heating device with a built-in temperature sensor, as shown in Fig. 26 (a). After activation, the strips were coated with a primer and embedded in a cementitious grout. In another field application, several shear-deficient RC beams of a cultural heritage theatre in Baden, Switzerland, were strengthened by U-shaped stirrups of activated Fe-SMA embedded in a sprayed mortar [105–106]. The bottom and side surfaces of the beams were first roughened by water jetting, and holes were drilled into the upper slab. The Fe-SMA stirrups were installed into the drilled holes, which were then filled with grout, as shown in Fig. 26 (b). The side surfaces were covered with sprayed mortar after the formwork was installed. The stirrups were finally activated using the resistive heating method after sufficient curing. Despite several successful field implementations, monitoring studies are recommended for SMA-strengthened structural components to ensure their long-term integrity and performance.

7. Challenges and future opportunities

There are certain challenges that need to be addressed before the widespread adoption of SMAs in RC structures. A detailed review of these challenges, along with future opportunities, is presented in this section.

(a)

(b)

Fig. 26. Field applications of activated Fe-SMA: (a) flexural strengthening of a concrete slab of a Kasinopark in Aarau, Switzerland, and (b) shear strengthening of RC beams of a theatre in Baden, Switzerland [106].

i) deterioration and shrinkage of cementitious matrix

An important aspect in utilizing the SME of SMAs is to ensure that the heating temperature required for the activation of SMAs does not damage the cementitious matrix of the concrete substrate. Generally, no microcracks have been reported in the cement matrix up to 200 °C; however, microcracks can start forming and propagate in the cement matrix if the temperature increases further. In addition, the compressive strength of concrete dramatically decreases if it is heated in the range of 300–800 °C [107]. Therefore, SMAs that can result in higher recovery stresses (greater than 500 MPa) at lower activation temperatures (<200 °C) are more suitable for strengthening applications of RC structures. Notably, the existing SMAs require an activation temperature not greater than 200 °C to generate recovery stresses. However, to obtain higher recovery stresses in the range of 400–500 MPa, heating to more than 200 °C becomes a requirement [64]. As for shrinkage, it has been observed in the previous studies that when SMA rebars are embedded in a shotcrete layer, shrinkage in shotcrete may lead to cracks, which in turn reduces the efficacy of the strengthening technique [51]. This issue needs to be addressed in future research.

ii) bond behavior with concrete

SMAs that are commonly manufactured have a smooth surface; therefore, the development of an adequate bond with the concrete substrate remains a challenge. This can cause problems when the SMAs are used as internal reinforcement instead of steel. Previous studies indicate that plain bars can have up to 30% less bond strength than ribbed bars [108–109]. Poor bonding with concrete can result in large crack widths, as reported in [32,34]. The bond behavior of smooth SMA rebars with concrete can be improved using SMA rebars with end hooks or by roughening the surface of SMA rebars through sandblasting [27]. Large-scale commercial manufacturing of ribbed SMA rebars can help resolve this issue. Recently, the bond behavior of ribbed Fe-SMA used as NSM and embedded rebars has been studied [75,79,81,115]. The outcome indicated that initial prestressing did not reduce the bond strength of the NSM SMA rebars with a full bond length. The required anchorage length to reach the tensile rupture of NSM SMA rebars was reported to be between 400 and 800 mm for less ductile and more than 800 mm for more ductile Fe-SMA rebars [79]. It is recommended that the cover depth be increased to avoid premature bond failure in the case of short bond lengths [81]. For embedded SMA rebars, the bond strength of unconfined specimens was found to decrease with the activation temperature, whereas the activation temperature had a negligible effect on the bond strength of the confined specimens. The bond strength of Fe-SMA rebars in confined specimens was reported to be 15% lower than that of conventional steel rebars [75]. More studies are still needed to investigate the SMA bond characteristics, especially for post-installed SMA rebars that are used in retrofit applications.

iii) corrosion resistance

The corrosion characteristics of SMA reinforcement may pose a challenge in effectively utilizing SMAs for upgrading deteriorating structures. Previous studies on various compositions of Fe-SMA have shown that a composition with 12% chromium exhibits corrosion performance similar to that of stainless steel, whereas the composition with 5% chromium displays poor corrosion behavior [110]. The Fe-SMA composition proposed in [111] and later implemented in a set of strengthening studies [50–52] is also expected to show an improved corrosion resistance owing to the presence of 10% chromium. However, this needs to be quantified in future studies. A high corrosion potential has been reported for Ni-Ti-Nb compared to Ni-Ti SMA [112], while Ni-Ti SMA exhibits satisfactory corrosion performance [113]. The corrosion characteristics of superelastic Cu-Al-Mn SMAs have not been investigated to date.

iv) recovery stress relaxation

The relaxation of recovery stress over time also needs to be studied in detail. Stress relaxation can be formulated into the design by including an appropriate reduction factor for the generated recovery stress. For example, the stress relaxation of Fe-SMA rebars was reported to be 10% after 2000 h (~83 days) [64]. An important aspect that should be particularly investigated is whether heating to the activation temperature in several steps results in a lower stress relaxation, as opposed to heating to the activation temperature in a single step. Further studies on this subject are required.

v) elastic modulus and stiffness

Because of the relatively low elastic modulus of the available Ni-Ti SMAs (compared to steel), the use of Ni-Ti SMA rebars as internal reinforcement (in place of steel) without compromising the stiffness of the structure remains challenging. A possible solution to address this issue is the partial replacement of steel with SMA rebars, as explored in a few previous studies [7,43]. Another option is the use of advanced materials that offer a high elastic modulus (e.g., ultra-high performance concrete) in conjunction with SMAs in the plastic hinge region of the target structural component. The elastic modulus of the as-received Fe-SMAs has been reported to be in the range of 165 GPa; however, on loading after activation, the elastic modulus of the Fe-SMA is approximately 75 GPa [64]. Yang et al. [104] attributed this behavior to a higher austenite-to-martensite phase transformation during the activation process. The smaller austenite to martensite phase transformation during the prestraining stage, in contrast, results in a higher axial modulus of the prestrained Fe-SMA compared to the as-received material.

vi) loading after activation

Studies on the behavior of activated SMAs under cyclic loading histories have shown a reduction in the prestressing force with increasing cyclic strains [66–67]. A subject that needs to be explored further is the behavior of SMAs upon loading after activation, particularly the effectiveness of prestressing under large reversals of tension and compression strains commonly observed during earthquake-induced excitations.

vii) Self-centering and other innovative applications

Previous research on the strengthening and self-centering of RC structures, particularly RC columns, beam-column joints, and walls, have mostly utilized superelastic Ni-based SMAs. However, no experimental study has so far exploited the SME of Fe-SMAs to axially or laterally prestress RC columns, beam-column joints, and walls. Considering that Fe-SMAs have been developed after the other SMA types, it is worthwhile to explore the effectiveness of Fe-SMAs in prestressing RC structures to improve their self-centering potential. Future research is also recommended for developing guidelines that can specify the amount of SMA longitudinal reinforcement required to ensure the self-centering of RC structures. Similarly, guidelines to specify an adequate amount of SMA transverse reinforcement are required to achieve effective confinement.

8. Conclusions

The comprehensive literature review presented in this paper shows that SMAs can be considered as a competitive alternative for strengthening and self-centering existing and new RC structures. The advantages of SMAs compared to conventional steel include excellent shape recovery and enhanced ductility, rapid and easy installation in the field, and a minimum friction loss and/or corrosion in the long term. The inclusion of superelastic SMAs (i.e., Ni-Ti and Cu-SMAs), as internal reinforcements (in place of steel), in new RC structural components can result in the reduction of residual displacements up to 90%, leading to self-centering behavior. However, the replacement of internal steel reinforcement with superelastic SMA rebars can result in low initial stiffness owing to the low elastic modulus of SMAs compared with that of conventional steel. The application of Fe-SMAs as internal reinforcements, mainly as prestressing elements, is deemed promising, as they exhibit a high elastic modulus. The issue of the low elastic modulus of Ni-Ti SMAs can be addressed by benefiting from some steel rebars in combination with Ni-Ti SMA rebars to maintain the expected stiffness while introducing the ability to partially recover the deformations. Otherwise, superelastic SMAs can be used in conjunction with advanced

construction materials that offer a high elastic modulus in the plastic hinge region of the structural components of interest. The use of such materials can also help to enhance the energy dissipation capacity of the structural components, which can be adversely affected by the flag-shaped hysteresis response of SMAs. Because of their low cost and good machinability, Cu-based SMAs have been recognized as a suitable choice for applications where the superelastic behavior of SMAs is critical.

The strengthening of RC structural components by exploiting the SME of Ni-Ti-Nb and Fe-SMA longitudinal reinforcements can result in enhanced stiffness and crack resistance, along with reduced deflection under extreme loads. Furthermore, the use of such SMAs leads to a reduction in residual displacements under cyclic loads. This can be particularly useful for adding self-centering behavior to an existing RC structure. For this purpose, activated SMAs can be utilized in the form of embedded or NSM reinforcements in existing RC columns, beams, beam-column joints, and shear walls. Thus, the SMA-equipped structural components can develop the ability to partially recover from their deformations under extreme loads, minimizing the need for repair activities. For this purpose, the selection of an optimum prestressing level is crucial, as the ductility of the structural components is reduced at a high prestressing force. The SME of SMAs has so far been used only for prestressing RC beams. Future studies are required to evaluate the feasibility of prestressing columns, beam-column joints, and walls by utilizing the SME of SMAs, particularly because of its ease of application compared to traditional prestressing techniques.

A comparison of different types of SMAs revealed that Fe-SMA is well-suited for applications where the SME needs to be exploited. This is because of its low cost, good machinability, high elastic modulus, and wide thermal hysteresis response. Fe-SMA is also a good candidate for prestressing, instead of steel or FRP tendons, because the recovery stress generated upon the thermal activation of Fe-SMA can lead to self-prestressing of the structural components of interest without the need for mechanical jacks, anchors, ducts, or hydraulic devices. In addition, owing to the uniform distribution of the tensile force along the full length of the SMA tendons (with negligible friction losses), they can be employed for prestressing both straight and curved RC structural components. In previous studies, the SME of SMA spirals was effectively utilized for the active confinement and shear strengthening of RC structural components. Strengthening with activated SMA spirals results in an enhanced ductility and energy dissipation capacity of RC structural components. In addition, the residual deformations were reduced by active confinement. The combined prestressing effect of longitudinal and transverse SMA reinforcements is an important research topic that can be further explored, especially to quantify how the residual deformations of the RC structural components can be further reduced.

With the unique capabilities introduced by SMAs for both new and existing structures, large-scale manufacturing of SMAs has significantly expanded, which is expected to further reduce the material costs in the future. Research on the use of SMAs for civil structures is still in the initial stages, and numerous aspects need to be understood in detail before SMAs can be widely adopted for practical applications. A few relevant aspects that require particular attention are the bond behavior of SMA reinforcement with concrete, stress relaxation over time, response to service loads after activation, especially tension–compression loading reversals, and integrity of the concrete substrate after the thermal activation of SMA. In addition, standard codes and guidelines need to be developed to specify the amount of SMA required for effective flexural and shear strengthening of RC structures.

Declaration of Competing Interest

The authors declare that they have no known competing financial interests or personal relationships that could have appeared to influence the work reported in this paper.

Acknowledgments

The financial support from the Swiss Innovation Agency under the grant no. 39259.1 IP-ENG and the Swiss National Science Foundation under the grant no. IZSEZ0_205347 for Scientific Exchanges is gratefully acknowledged.

References

[1] S. Raza, M.K.I. Khan, S.J. Menegon, H.-H. Tsang, J.L. Wilson, Strengthening and repair of reinforced concrete columns by jacketing: State-of-the-art review, Sustainability 11 (11) (2019) 3208, https://doi.org/10.3390/su11113208.
[2] M. Engindeniz, L.F. Kahn, A.H. Zureick, Repair and strengthening of reinforced concrete beam-column joints: state of the art, ACI Structural Journal 102 (2) (2005), https://doi.org/10.14359/14269.
[3] L.N. Koutas, Z. Tetta, D.A. Bournas, T.C. Triantafillou, Strengthening of concrete structures with textile reinforced mortars: state-of-the-art review, Journal of Composites for Construction 23 (1) (2019) 03118001, https://doi.org/10.1061/(ASCE)CC.1943-5614.0000882.
[4] A. Siddika, M.A.A. Mamun, R. Alyousef, Y.H.M. Amran, Strengthening of reinforced concrete beams by using fiber-reinforced polymer composites: A review, Journal of Building Engineering 25 (2019) 100798, https://doi.org/10.1016/j.jobe.2019.100798.
[5] C. Czaderski, M. Shahverdi, R. Bronnimann, C. Leinenbach, M. Motavalli, Feasibility of iron-based shape memory alloy strips for prestressed strengthening of concrete structures, Construction and Building Materials 56 (2014) 94–105, https://doi.org/10.1016/j.conbuildmat.2014.01.069.
[6] S. Zareie, A.S. Issa, R.J. Seethaler, A. Zabihollah, Recent advances in the applications of shape memory alloys in civil infrastructures: A review, Structures 27 (2020) 1535–1550, https://doi.org/10.1016/j.istruc.2020.05.058.
[7] F. Hosseini, B. Gencturk, S. Lahpour, D.I. Gil, An experimental investigation of innovative bridge columns with engineered cementitious composites and cu-al-mn super-elastic alloys, Smart Materials and Structures 24 (8) (2015) 085029, https://doi.org/10.1088/0964-1726/24/8/085029.
[8] L. Janke, C. Czaderski, M. Motavalli, J. Ruth, Applications of shape memory alloys in civil engineering structures—Overview, limits and new ideas, Materials and Structures 38 (5) (2005) 578–592, https://doi.org/10.1007/BF02479550.
[9] G. Song, N. Ma, H.N. Li, Applications of shape memory alloys in civil structures, Engineering Structures 28 (9) (2006) 1266–1274, https://doi.org/10.1016/j.engstruct.2005.12.010.
[10] O.E. Ozbulut, S. Hurlebaus, R. Desroches, Seismic Response Control Using Shape Memory Alloys: A Review, Journal of Intelligent Material Systems and Structures 22 (14) (2011) 1531–1549, https://doi.org/10.1177/1045389X11411220.
[11] J.J. Mohd, M. Leary, A. Subic, M.A. Gibson, A review of shape memory alloy research, applications and opportunities, Materials & Design 1980–2015 (56) (2014) 1078–1113, https://doi.org/10.1016/j.matdes.2013.11.084.
[12] R. DesRoches, J. McCormick, M. Delemont, Cyclic properties of superelastic shape memory alloy wires and bars, Journal of Structural Engineering 130 (1) (2004) 38–46, https://doi.org/10.1061/(ASCE)0733-9445(2004)130:1(38).
[13] J. McCormick, J. Tyber, R. DesRoches, K. Gall, J. Maier Hans, Structural Engineering with NiTi. II: Mechanical Behavior and Scaling, Journal of Engineering Mechanics 133 (9) (2007) 1019–1029, https://doi.org/10.1061/(ASCE)0733-9399(2007)133:9(1019).
[14] Y. Araki, T. Endo, T. Omori, Y. Sutou, Y. Koetaka, R. Kainuma, K. Ishida, Potential of superelastic Cu–Al–Mn alloy bars for seismic applications, Earthquake Engineering & Structural Dynamics 40 (1) (2011) 107–115, https://doi.org/10.1002/eqe.v40.110.1002/eqe.1029.
[15] H. Li, Z.Q. Liu, J.P. Ou, Experimental study of a simple reinforced concrete beam temporarily strengthened by sma wires followed by permanent strengthening with cfrp plates, Engineering Structures 30 (3) (2008) 716–723, https://doi.org/10.1016/j.engstruct.2007.05.020.
[16] E. Choi, Y.S. Chung, D.H. Choi, R. DesRoches, Seismic protection of lap-spliced rc columns using sma wire jackets, Magazine of Concrete Research 64 (3) (2012) 239–252, https://doi.org/10.1680/macr.10.00181.
[17] M. Shin, B. Andrawes, Emergency repair of severely damaged reinforced concrete columns using active confinement with shape memory alloys, Smart Materials & Structures 20 (6) (2011) 065018, https://doi.org/10.1088/0964-1726/20/6/065018.
[18] Z.C. Deng, Q.B. Li, H.J. Sun, Behavior of concrete beam with embedded shape memory alloy wires, Engineering Structures 28 (12) (2006) 1691–1697, https://doi.org/10.1016/j.engstruct.2006.03.002.
[19] M.S. Saiidi, M. Sadrossadat-Zadeh, C. Ayoub, A. Itani, Pilot study of behavior of concrete beams reinforced with shape memory alloys, Journal of Materials in Civil Engineering 19 (6) (2007) 454–461, https://doi.org/10.1061/(asce)0899-1561(2007)19:6(454).
[20] Y. Kuang, J. Ou, Self-repairing performance of concrete beams strengthened using superelastic sma wires in combination with adhesives released from hollow fibers, Smart Materials and Structures 17 (2) (2008) 025020, https://doi.org/10.1088/0964-1726/17/2/025020.
[21] B. Mas, A. Cladera, C. Ribas, Experimental study on concrete beams reinforced with pseudoelastic ni-ti continuous rectangular spiral reinforcement failing in shear, Engineering Structures 127 (2016) 759–768, https://doi.org/10.1016/j.engstruct.2016.09.022.

[22] F. Azadpour, A.A. Maghsoudi, Experimental and analytical investigation of continuous rc beams strengthened by sma strands under cyclic loading, Construction and Building Materials 239 (2020) 117730, https://doi.org/10.1016/j.conbuildmat.2019.117730.
[23] M.S. Saiidi, H.Y. Wang, Exploratory study of seismic response of concrete columns with shape memory alloys reinforcement, Aci Structural Journal 103 (3) (2006) 436–443.
[24] M.S. Saiidi, M. O'Brien, M. Sadrossadat-Zadeh, Cyclic response of concrete bridge columns using superelastic nitinol and bendable concrete, Aci Structural Journal 106 (1) (2009) 69–77.
[25] C.A.C. Noguez, M.S. Saiidi, Shake-table studies of a four-span bridge model with advanced materials, Journal of Structural Engineering-Asce 138 (2) (2012) 182–191, https://doi.org/10.1061/(asce)st.1943-541x.0000457.
[26] M. Tazarv, M. Saiid Saiidi, Low-damage precast columns for accelerated bridge construction in high seismic zones, Journal of Bridge Engineering 21 (3) (2016) 04015056, https://doi.org/10.1061/(ASCE)BE.1943-5592.0000806.
[27] G. Xing, O.E. Ozbulut, M.A. Al-Dhabyani, Z. Chang, S.M. Daghash, Enhancing flexural capacity of rc columns through near surface mounted sma and cfrp bars, Journal of Composite Materials 54 (29) (2020) 4661–4676, https://doi.org/10.1177/0021998320937054.
[28] M.A. Youssef, M.S. Alam, M. Nehdi, Experimental investigation on the seismic behavior of beam-column joints reinforced with superelastic shape memory alloys, Journal of Earthquake Engineering 12 (7) (2008) 1205–1222, https://doi.org/10.1080/13632460802003082.
[29] M. Nehdi, M.S. Alam, M.A. Youssef, Development of corrosion-free concrete beam-column joint with adequate seismic energy dissipation, Engineering Structures 32 (9) (2010) 2518–2528, https://doi.org/10.1016/j.engstruct.2010.04.020.
[30] M. Nehdi, M.S. Alam, M.A. Youssef, Seismic behaviour of repaired superelastic shape memory alloy reinforced concrete beam-column joint, Smart Structures and Systems 7 (5) (2011) 329–348, https://doi.org/10.12989/sss.2011.7.5.329.
[31] F. Oudah, R. El-Hacha, Joint performance in concrete beam-column connections reinforced using sma smart material, Engineering Structures 151 (2017) 745–760, https://doi.org/10.1016/j.engstruct.2017.08.054.
[32] F. Oudah, R. El-Hacha, Innovative self-centering concrete beam-column connection reinforced using shape memory alloy, Aci Structural Journal 115 (3) (2018) 607–620, https://doi.org/10.14359/51702132.
[33] O. Yurdakul, O. Tunaboyu, O. Avsar, Retrofit of non-seismically designed beam-column joints by post-tensioned superelastic shape memory alloy bars, Bulletin of Earthquake Engineering 16 (11) (2018) 5279–5307, https://doi.org/10.1007/s10518-018-0323-y.
[34] A. Abdulridha, D. Palermo, Behaviour and modelling of hybrid sma-steel reinforced concrete slender shear wall, Engineering Structures 147 (2017) 77–89, https://doi.org/10.1016/j.engstruct.2017.04.058.
[35] L. Cortes-Puentes, M. Zaidi, D. Palermo, E. Dragomirescu, Cyclic loading testing of repaired sma and steel reinforced concrete shear walls, Engineering Structures 168 (2018) 128–141, https://doi.org/10.1016/j.engstruct.2018.04.044.
[36] W.L. Cortés-Puentes, D. Palermo, Seismic retrofit of concrete shear walls with sma tension braces, Journal of Structural Engineering 144 (2) (2018) 04017200, https://doi.org/10.1061/(ASCE)ST.1943-541X.0001936.
[37] M.J. Tolou Kian, C. Cruz-Noguez, Reinforced concrete shear walls detailed with innovative materials: Seismic performance, Journal of Composites for Construction 22 (6) (2018) 04018052, https://doi.org/10.1061/(ASCE)CC.1943-5614.0000893.
[38] J.P.d. Almeida, M. Steinmetz, F. Rigot, S. de Cock, Shape-memory niti alloy rebars in flexural-controlled large-scale reinforced concrete walls: Experimental investigation on self-centring and damage limitation, Engineering Structures 220 (2020) 110865, https://doi.org/10.1016/j.engstruct.2020.110865.
[39] J.M. Rius, A. Cladera, C. Ribas, B. Mas, Shear strengthening of reinforced concrete beams using shape memory alloys, Construction and Building Materials 200 (2019) 420–435, https://doi.org/10.1016/j.conbuildmat.2018.12.104.
[40] A. Sinha, N. Tatar, J. Tatar, Rapid heat-activated post-tensioning of damaged reinforced concrete girders with unbonded near-surface mounted (nsm) nitinb shape-memory alloy wires, Materials and Structures 53 (4) (2020), https://doi.org/10.1617/s11527-020-01522-8.
[41] M. Shin, B. Andrawes, Lateral cyclic behavior of reinforced concrete columns retrofitted with shape memory spirals and frp wraps, Journal of Structural Engineering 137 (11) (2011) 1282–1290, https://doi.org/10.1061/(asce)st.1943-541x.0000364.
[42] D. Jung, J. Wilcoski, B. Andrawes, Bidirectional shake table testing of rc columns retrofitted and repaired with shape memory alloy spirals, Engineering Structures 160 (2018) 171–185, https://doi.org/10.1016/j.engstruct.2017.12.046.
[43] K.C. Shrestha, Y. Araki, T. Nagae, Y. Koetaka, Y. Suzuki, T. Omori, Y. Sutou, R. Kainuma, K. Ishida, Feasibility of cu-al-mn superelastic alloy bars as reinforcement elements in concrete beams, Smart Materials and Structures 22 (2) (2013) 025025, https://doi.org/10.1088/0964-1726/22/2/025025.
[44] S. Pareek, K.C. Shrestha, Y. Suzuki, T. Omori, R. Kainuma, Y. Araki, Feasibility of externally activated self-repairing concrete with epoxy injection network and cu-al-mn superelastic alloy reinforcing bars, Smart Materials and Structures 23 (10) (2014) 105027, https://doi.org/10.1088/0964-1726/23/10/105027.
[45] S. Pareek, Y. Suzuki, Y. Araki, M.A. Youssef, M. Meshaly, Plastic hinge relocation in reinforced concrete beams using cu-al-mn sma bars, Engineering Structures 175 (2018) 765–775, https://doi.org/10.1016/j.engstruct.2018.08.072.
[46] S. Varela, M. Saiidi, Resilient deconstructible columns for accelerated bridge construction in seismically active areas, Journal of Intelligent Material Systems and Structures 28 (13) (2017) 1751–1774, https://doi.org/10.1177/1045389x16679285.
[47] B. Gencturk, Y. Araki, T. Kusama, T. Omori, R. Kainuma, F. Medina, Loading rate and temperature dependency of superelastic Cu–Al–Mn alloys, Construction and Building Materials 53 (2014) 555–560, https://doi.org/10.1016/j.conbuildmat.2013.12.002.
[48] J. Michels, M. Shahverdi, C. Czaderski, Flexural strengthening of structural concrete with iron-based shape memory alloy strips, Structural Concrete 19 (3) (2018) 876–891, https://doi.org/10.1002/suco.2018.19.issue-310.1002/suco.201700120.
[49] P. Soroushian K. Ostowari A. Nossoni H. Chowdhury 1770 1 2001 20 26.
[50] M. Shahverdi, C. Czaderski, M. Motavalli, Iron-based shape memory alloys for prestressed near-surface mounted strengthening of reinforced concrete beams, Construction and Building Materials 112 (2016) 28–38, https://doi.org/10.1016/j.conbuildmat.2016.02.174.
[51] M. Shahverdi, C. Czaderski, P. Annen, M. Motavalli, Strengthening of rc beams by iron-based shape memory alloy bars embedded in a shotcrete layer, Engineering Structures 117 (2016) 263–273, https://doi.org/10.1016/j.engstruct.2016.03.023.
[52] H. Rojob, R. El-Hacha, Self-prestressing using iron-based shape memory alloy for flexural strengthening of reinforced concrete beams, Aci Structural Journal 114 (2) (2017) 523–532, https://doi.org/10.14359/51689455.
[53] R. El-Hacha, H. Rojob, Flexural strengthening of large-scale reinforced concrete beams using near-surface -mounted self-prestressed iron-based shape-memory alloy strips, Pci Journal (2018) 55–65.
[54] H. Rojob, R. El-Hacha, Fatigue performance of rc beams strengthened with self-prestressed iron-based shape memory alloys, Engineering Structures 168 (2018) 35–43, https://doi.org/10.1016/j.engstruct.2018.04.042.
[55] K. Hong, S. Lee, Y. Yeon, K. Jung, Flexural response of reinforced concrete beams strengthened with near-surface-mounted fe-based shape-memory alloy strips. International Journal of Concrete, Structures and Materials 12 (1) (2018), https://doi.org/10.1186/s40069-018-0279-y.
[56] L.A. Montoya-Coronado, J.G. Ruiz-Pinilla, C. Ribas, A. Cladera, Experimental study on shear strengthening of shear critical rc beams using iron-based shape memory alloy strips, Engineering Structures 200 (2019) 109680, https://doi.org/10.1016/j.engstruct.2019.109680.
[57] E. Strieder, C. Aigner, G. Petautschnig, S. Horn, M. Marcon, M. Schwenn, O. Zeman, P. Castillo, R. Wan-Wendner, K. Bergmeister, Strengthening of reinforced concrete beams with externally mounted sequentially activated iron-based shape memory alloys, Materials 12 (3) (2019) 345, https://doi.org/10.3390/ma12030345.
[58] A. Cladera, L.A. Montoya-Coronado, J.G. Ruiz-Pinilla, C. Ribas, Shear strengthening of slender reinforced concrete t-shaped beams using iron-based shape memory alloy strips, Engineering Structures 221 (2020) 111018, https://doi.org/10.1016/j.engstruct.2020.111018.
[59] S. Yan, M.Y. Lin, Z.F. Xiao, J. Niu, Experimental research on resilient performances of fe-based sma-reinforced concrete shear walls, IOP Conference Series: Earth and Environmental Science 189 (2018), 032028, https://doi.org/10.1088/1755-1315/189/3/032028.
[60] A. Cladera, B. Weber, C. Leinenbach, C. Czaderski, M. Shahverdi, M. Motavalli, Iron-based shape memory alloys for civil engineering structures: An overview, Construction and Building Materials 63 (2014) 281–293, https://doi.org/10.1016/j.conbuildmat.2014.04.032.
[61] J. Michels, M. Shahverdi, C. Czaderski, R. El-Hacha, Mechanical performance of iron-based shape-memory alloy ribbed bars for concrete prestressing, Aci Materials Journal 115 (6) (2018) 877–886, https://doi.org/10.14359/51710959.
[62] E. Choi, B. Mohammadzadeh, H.S. Kim, Sma bending bars as self-centering and damping devices, Smart Materials and Structures 28 (2) (2019) 025029, https://doi.org/10.1088/1361-665X/aaf5e3.
[63] K.A. Tsoi, R. Stalmans, J. Schrooten, Transformational behaviour of constrained shape memory alloys, Acta Materialia 50 (14) (2002) 3535–3544, https://doi.org/10.1016/s1359-6454(02)00145-3.
[64] M. Shahverdi, J. Michels, C. Czaderski, M. Motavalli, Iron-based shape memory alloy strips for strengthening rc members: Material behavior and characterization, Construction and Building Materials 173 (2018) 586–599, https://doi.org/10.1016/j.conbuildmat.2018.04.057.
[65] E. Choi, T.H. Nam, Y.S. Chung, Y.W. Kim, S.Y. Lee, Behavior of NiTiNb SMA wires under recovery stress or prestressing, Nanoscale research letters 7 (1) (2012) 66, https://doi.org/10.1186/1556-276X-7-66.
[66] E. Ghafoori, E. Hosseini, C. Leinenbach, J. Michels, M. Motavalli, Fatigue behavior of a Fe-Mn-Si shape memory alloy used for prestressed strengthening, Materials & Design 133 (2017) 349–362, https://doi.org/10.1016/j.matdes.2017.07.055.
[67] E. Hosseini, E. Ghafoori, C. Leinenbach, M. Motavalli, S.R. Holdsworth, Stress recovery and cyclic behaviour of an Fe-Mn-Si shape memory alloy after multiple thermal activation, Smart Materials and Structures 27 (2) (2018) 10, https://doi.org/10.1088/1361-665X/aaa2c9.
[68] D.I.H. Rosa, A. Hartloper, A. de Castro e Sousa, D.G. Lignos, M. Motavalli, E. Ghafoori, Experimental behavior of iron-based shape memory alloys under cyclic loading histories, Construction and Building Materials 272 (2021) 121712, https://doi.org/10.1016/j.conbuildmat.2020.121712.
[69] Y. Yang, A. Arabi-Hashemi, C. Leinenbach, M. Shahverdi, Influence of thermal treatment conditions on recovery stress formation in an FeMnSi-SMA, Materials Science and Engineering: A 802 (2021) 140694, https://doi.org/10.1016/j.msea.2020.140694.

[70] K. Uchida, N. Shigenaka, T. Sakuma, Y. Sutou, K. Yamauchi, Effects of Pre-Strain and Heat Treatment Temperature on Phase Transformation Temperature and Shape Recovery Stress of Ti-Ni-Nb Shape Memory Alloys for Pipe Joint Applications, Materials Transactions 49 (7) (2008) 1650–1655, https://doi.org/10.2320/matertrans.MRA2007266.

[71] Y.I. Yoo, J.W. Jeong, J.J. Lee, C.H. Lee, Effect of heat treatment on the two-way recovery stress of tube-shaped NiTi, Journal of Intelligent Material Systems and Structures. 23 (10) (2012) 1161–1168, https://doi.org/10.1177/1045389X12444489.

[72] J.-l. Liu, H.-Y. Huang, J.-X. Xie, Effects of aging treatment on the microstructure and superelasticity of columnar-grained Cu71Al18Mn11 shape memory alloy, International Journal of Minerals, Metallurgy, and Materials. 23 (10) (2016) 1157–1166, https://doi.org/10.1007/s12613-016-1335-8.

[73] I. Ferretto, D. Kim, N.M. Della Ventura, M. Shahverdi, W. Lee, C. Leinenbach, Laser powder bed fusion of a Fe–Mn–Si shape memory alloy, Additive Manufacturing 46 (2021) 102071, https://doi.org/10.1016/j.addma.2021.102071.

[74] E. Ghafoori, M. Neuenschwander, M. Shahverdi, C. Czaderski, M. Fontana, Elevated temperature behavior of an iron-based shape memory alloy used for prestressed strengthening of civil structures, Construction and Building Materials 211 (2019) 437–452, https://doi.org/10.1016/j.conbuildmat.2019.03.098.

[75] G. Fawaz, J. Murcia-Delso, Bond behavior of iron-based shape memory alloy reinforcing bars embedded in concrete, Materials and Structures 53 (5) (2020) 114, https://doi.org/10.1617/s11527-020-01548-y.

[76] U. Diederichs, U. Schneider, Bond strength at high temperatures, Magazine of Concrete Research 33 (115) (1981) 75–84, https://doi.org/10.1680/macr.1981.33.115.75.

[77] K. Hertz, The anchorage capacity of reinforcing bars at normal and high temperatures, Magazine of Concrete Research 34 (121) (1982) 213–220, https://doi.org/10.1680/macr.1982.34.121.213.

[78] P.D. Morley, R. Royles, Response of the Bond in Reinforced Concrete to High Temperatures, Magazine of Concrete Research 35 (123) (1983) 67–74, https://doi.org/10.1680/macr.1983.35.123.67.

[79] B. Schranz, C. Czaderski, T. Vogel, M. Shahverdi, Bond investigations of prestressed, near-surface-mounted, ribbed memory-steel bars with full bond length, Materials & Design 196 (2020) 109145, https://doi.org/10.1016/j.matdes.2020.109145.

[80] T. Pothisiri, P. Panedpojaman, Modeling of bonding between steel rebar and concrete at elevated temperatures, Construction and Building Materials 27 (1) (2012) 130–140, https://doi.org/10.1016/j.conbuildmat.2011.08.014.

[81] B. Schranz, C. Czaderski, T. Vogel, M. Shahverdi, Bond behaviour of ribbed near-surface-mounted iron-based shape memory alloy bars with short bond lengths, Materials & Design 191 (2020) 108647, https://doi.org/10.1016/j.matdes.2020.108647.

[82] S.M. Daghash, O.E. Ozbulut, Bond–slip behavior of superelastic shape memory alloys for near-surface-mounted strengthening applications, Smart Materials and Structures 26 (3) (2017) 035020, https://doi.org/10.1088/1361-665X/26/3/035020.

[83] K. Hong, S. Lee, Han, & S., Yeon, Y, Evaluation of Fe-Based Shape Memory Alloy (Fe-SMA) as Strengthening Material for Reinforced Concrete Structures, Applied Sciences 8 (5) (2018) 730.

[84] M. Shahverdi, C. Czaderski, Long-term behavior of reinforced concrete beams strengthened by iron-based shape memory alloy strips. In: SMAR 2019—fifth conference on smart monitoring, assessment and rehabilitation of civil structures, 2019.

[85] K. Dommer, B. Andrawes, Thermomechanical characterization of NiTiNb shape memory alloy for concrete active confinement applications, Journal of Materials in Civil Engineering 24 (10) (2012) 1274–1282, https://doi.org/10.1061/(ASCE)MT.1943-5533.0000495.

[86] A. Abdulridha, D. Palermo, S. Foo, F.J. Vecchio, Behavior and modeling of superelastic shape memory alloy reinforced concrete beams, Engineering Structures 49 (2013) 893–904, https://doi.org/10.1016/j.engstruct.2012.12.041.

[87] S. Abouali, M. Shahverdi, M. Ghassemieh, M. Motavalli, Nonlinear simulation of reinforced concrete beams retrofitted by near-surface mounted iron-based shape memory alloys, Engineering Structures 187 (2019) 133–148, https://doi.org/10.1016/j.engstruct.2019.02.060.

[88] N. Dolatabadi, M. Shahverdi, M. Ghassemieh, M. Motavalli, RC structures strengthened by an iron-based shape memory alloy embedded in a shotcrete layer—nonlinear finite element modeling, Materials. 13 (23) (2020) 5504, https://doi.org/10.3390/ma13235504.

[89] Bernhard Schranz, Julien Michels, Christoph Czaderski, Masoud Motavalli, Thomas Vogel, Moslem Shahverdi, Strengthening and prestressing of bridge decks with ribbed iron-based shape memory alloy bars, Engineering Structures 241 (2021) 112467, https://doi.org/10.1016/j.engstruct.2021.112467.

[90] Moein Rezapour, Mehdi Ghassemieh, Masoud Motavalli, Moslem Shahverdi, Numerical Modeling of Unreinforced Masonry Walls Strengthened with Fe-Based Shape Memory Alloy Strips, Materials 14 (11) (2021) 2961, https://doi.org/10.3390/ma14112961.

[91] E. Effendy, W.I. Liao, G. Song, Y.L. Mo, C.H. Loh, Seismic behavior of low-rise shear walls with sma bars, Earth & Space 2006 (2006) 1–8, https://doi.org/10.1061/40830(188)137.

[92] B. Mas, D. Biggs, I. Vieito, A. Cladera, J. Shaw, F. Martínez-Abella, Superelastic shape memory alloy cables for reinforced concrete applications, Construction and Building Materials 148 (2017) 307–320, https://doi.org/10.1016/j.conbuildmat.2017.05.041.

[93] C. Fang, Y. Zheng, J. Chen, M.C.H. Yam, W. Wang, Superelastic NiTi SMA cables: Thermal-mechanical behavior, hysteretic modelling and seismic application, Engineering Structures 183 (2019) 533–549, https://doi.org/10.1016/j.engstruct.2019.01.049.

[94] Yifei Shi, Hui Qian, Liping Kang, Zongao Li, Like Xia, Cyclic behavior of superelastic SMA cable and its application in an innovative self-centering BRB, Smart Materials and Structures 30 (9) (2021) 095019, https://doi.org/10.1088/1361-665X/ac1907.

[95] Fei Shi, Yun Zhou, Osman E. Ozbulut, Fengming Ren, Hysteretic response and failure behavior of an SMA cable-based self-centering brace, Structural Control and Health Monitoring 29 (1) (2022), https://doi.org/10.1002/stc.v29.110.1002/stc.2847.

[96] Christoph Czaderski, Moslem Shahverdi, Julien Michels, Iron based shape memory alloys as shear reinforcement for bridge girders, Construction and Building Materials 274 (2021) 121793, https://doi.org/10.1016/j.conbuildmat.2020.121793.

[97] Sebastian Varela, M 'Saiid' Saiidi, A bridge column with superelastic niti sma and replaceable rubber hinge for earthquake damage mitigation, Smart Materials and Structures 25 (7) (2016) 075012, https://doi.org/10.1088/0964-1726/25/7/075012.

[98] Fadi Oudah, Raafat El-Hacha, Monolithic SMA-reinforced double slotted beam-column connection, Smart Materials and Structures 29 (3) (2020) 035002, https://doi.org/10.1088/1361-665X/ab62df.

[99] Saiidi, M., M. Tazarv, S. Varela, S. Bennion, M. Marsh, I. Ghorbani, and T. Murphy (2017a). Seismic Evaluation of Bridge Columns with Energy Dissipating Mechanisms, Volume 1 –Research Overview. National Cooperative Highway Research Program, NCHRP Report 864, Transportation Research Board, Washington, DC.

[100] Saiidi, M., M. Tazarv, S. Varela, S. Bennion, M. Marsh, I. Ghorbani, and T. Murphy (2017b). Seismic Evaluation of Bridge Columns with Energy Dissipating Mechanisms, Volume 2 –Guidelines. National Cooperative Highway Research Program, NCHRP Report 864, Transportation Research Board, Washington, DC.

[101] AASHTO, AASHTO Guide Specifications for LRFD Seismic Bridge Design, American Association of State Highway and Transportation Officials, Washington, D.C., 2011.

[102] A.H.M.M. Billah, M.S. Alam, Performance-Based Seismic Design of Shape Memory Alloy–Reinforced Concrete Bridge Piers. I: Development of Performance-Based Damage States, Journal of Structural Engineering 142 (12) (2016) 04016140, https://doi.org/10.1061/(ASCE)ST.1943-541X.0001458.

[103] A.H.M.M. Billah, M.S. Alam, Performance-Based Seismic Design of Shape Memory Alloy-Reinforced Concrete Bridge Piers. II: Methodology and Design Example, Journal of Structural Engineering 142 (12) (2016) 04016141, https://doi.org/10.1061/(ASCE)ST.1943-541X.0001623.

[104] Y. Yang, M. Breveglieri, M. Shahverdi, Effect of Phase Changes on the Axial Modulus of an FeMnSi-Shape Memory Alloy, Retrieved from, Materials 14 (17) (2021) 4815, https://www.mdpi.com/1996-1944/14/17/4815.

[105] Schranz, B., Michels, J., Shahverdi, M., & Czaderski, C. (2019). Strengthening of concrete structures with iron-based shape memory alloy elements: case studies. 5th SMAR Conference, Potsdam, Germany.

[106] re-fer AG, Online product portfolio From 2020 https://www.re-fer.eu/en/references.

[107] Q. Ma, R. Guo, Z. Zhao, Z. Lin, K. He, Mechanical properties of concrete at high temperature—A review, Construction and Building Materials 93 (2015) 371–383, https://doi.org/10.1016/j.conbuildmat.2015.05.131.

[108] Y.L. Mo, J. Chan, Bond and slip of plain rebars in concrete, Journal of Materials in Civil Engineering. 8 (4) (1996) 208–211, https://doi.org/10.1061/(ASCE)0899-1561(1996)8:4(208).

[109] G.M. Verderame, G.D. Carlo, P. Ricci, G. Fabbrocino, Cyclic bond behavior of plain bars. Part II: Analytical investigation, Construction and Building Materials 23 (12) (2009) 3512–3522, https://doi.org/10.1016/j.conbuildmat.2009.07.001.

[110] H.C. Lin, K.M. Lin, C.S. Lin, T.M. Ouyang, The corrosion behavior of Fe-based shape memory alloys, Corrosion Science 44 (9) (2002) 2013–2026, https://doi.org/10.1016/S0010-938X(02)00027-6.

[111] Zhizhong Dong, Ulrich E. Klotz, Christian Leinenbach, Andrea Bergamini, Christoph Czaderski, Masoud Motavalli, A novel Fe-Mn-Si shape memory alloy with improved shape recovery properties by VC precipitation, Advanced Engineering Materials 11 (1-2) (2009) 40–44, https://doi.org/10.1002/adem.v11:1/210.1002/adem.200800312.

[112] K. Li, Y. Li, X. Huang, D. Gibson, Y. Zheng, J. Liu, Lu. Sun, Fu, Y. Q, Surface microstructures and corrosion resistance of Ni-Ti-Nb shape memory thin films, Applied Surface Science 414 (2017) 63–67, https://doi.org/10.1016/j.apsusc.2017.04.070.

[113] C. Velmurugan, V. Senthilkumar, P.S. Kamala, Microstructure and corrosion behavior of NiTi shape memory alloys sintered in the SPS process, International Journal of Minerals, Metallurgy, and Materials 26 (10) (2019) 1311–1321, https://doi.org/10.1007/s12613-019-1836-3.

[114] J. McCormick H. Aburano M. Ikenaga M. Nakashima Permissible residual deformation levels for building structures considering both safety and human elements 2008 Beijing, China.

[115] Bernhard Schranz, Miguel F. Nunes, Christoph Czaderski, Moslem Shahverdi, Fibre optic strain measurements for bond modelling of prestressed near-surface-mounted iron-based shape memory alloy bars, Construction and Building Materials 288 (2021) 123102, https://doi.org/10.1016/j.conbuildmat.2021.123102.